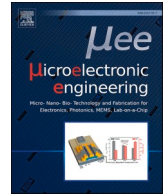




Contents lists available at ScienceDirect

Microelectronic Engineering

journal homepage: www.elsevier.com/locate/mee

Review article

Recent advances in micro- and bio- electromechanical system architectures for energy efficient chemiresistors

Bharat Sharma^{a,*}, Mukesh Kumar^b, Ashutosh Sharma^{c,d,**}^a Institute of Microstructure Technology, Karlsruhe Institute of Technology, Hermann-Von-Helmholtz-Platz 1, Eggenstein-Leopoldshafen 76344, Germany^b Department of Physics, Faculty of Science, Shree Guru Gobind Singh Tricentenary University, Gurugram 122505, Delhi-NCR, India^c Amity Institute of Applied Sciences, Amity University Jharkhand, Ranchi 834002, India^d Department of Materials Science and Engineering, Ajou University, 206-Worldcup-ro, Yeongtong-gu, Suwon 16499, Gyeonggi-do, Republic of Korea

ARTICLE INFO

Keywords:

Chemiresistors
Toxicity
Gas
Selectivity
Chemisorption

ABSTRACT

The recent evolution of microelectromechanical systems (MEMS) presents a more mature technology that expands from pure research towards multidisciplinary nanoelectromechanical systems (NEMS) research. The smaller size of NEMS makes them multifunctional, fast, energy-saving, and sensitive to any external stimuli. The extreme sensitivity of these NEMS opens new avenues to the various industrial sector of applications in bio-sensing, gas sensing, and medical implants which won't be possible with traditional MEMS counterparts. Most of the resistive-gas sensors are more popular than others but their elevated working temperatures consume more energy and limit their real-world applications. Various self-heating, embedded MEMS microheaters, and materials have been explored to improve the sensing performance. Thus, there is an urgent need of the hour to review the associated manufacturing techniques and evolution of MEMS fabrication for energy-saving gas sensors and new developments in this area. We overview the various manufacturing process and developments in MEMS/NEMS for gas sensor applications, and their historical perspectives, and provide future guidelines to meet the existing challenges for real-world gas sensing applications.

1. Introduction

In the past few eras, MEMS technology has unfurled innovative pathways in numerous applications including gas sensors and biosensors. MEMS-based devices were initially anticipated in the 1960s ensuring studies of the piezoresistive potential of silicon (Si) and germanium (Ge). The expansion in this area gradually clambered up in the 1980s. MEMS-based devices propose features such as scalable devices, small size, and reduction in cost as compared to conventional engineering approaches. Lately, micro- and nanofabrication approaches have been extensively used to design and fabricate MEMS/NEMS-based gas sensors for a variety of applications in environmental sensing, physical activities, healthcare, and safety [1–3]. The behavior of the active components in NEMS are often in the form of doubly clamped beams or cantilevers with nanoscale diameters. These active components are made of a variety of materials, including silicon, carbon nanotubes, silicon carbide, gold, and platinum. The building block of

integrated circuits and MEMS microelectronic devices have been widely relied on silicon semiconductors. NEMS-based miniaturized gas sensors can attain high resolution, and promise a reduction in cost as compared to conventional sensing devices [4]. This is due to the fact that the thickness of the membrane can go as thin as possible when utilizing nanoscale sensitive materials—often has a significant impact on the sensitivity and performance of NEMS sensors. When it comes to mechanical biosensors, NEMS offer three key benefits. Firstly, they can operate at the nanogram scale for mass resolution in fluid media. Second, they are highly mechanically compliant, the ability of a NEMS device to be displaced or deformed easily to measure a differentiable displacement. For instance, NEMS sensors are sensitive enough to detect the breakage of hydrogen bonds as they can resolve forces as low as 10 pN. Third, quick response times from small fluidic mechanical devices could make it easier to monitor biological processes in real time [5].

Given these essential benefits, MEMS-based gas sensors are utilized widely in numerous applications such as navigation sensing on

* Corresponding author at: Institute of Microstructure Technology, Karlsruhe Institute of Technology, Hermann-Von-Helmholtz-Platz 1, Eggenstein-Leopoldshafen 76344, Germany.

** Corresponding author at: Department of Materials Science and Engineering, 206-Worldcup-ro, Yeongtong-gu, Suwon 16499, Gyeonggi-do, Republic of Korea.
E-mail addresses: bharatsharma796@gmail.com (B. Sharma), stannum.ashu@gmail.com (A. Sharma).

<https://doi.org/10.1016/j.mee.2024.112168>

Received 6 June 2023; Received in revised form 5 January 2024; Accepted 26 February 2024

Available online 28 February 2024

0167-9317/© 2024 The Authors. Published by Elsevier B.V. This is an open access article under the CC BY license (<http://creativecommons.org/licenses/by/4.0/>).

autonomous underwater vehicles (AUV) [6], automobiles, diagnostic devices, [7], gas monitoring structures, chemistry, and therapeutic fields. There is a great need for miniaturization, portability, and reduced power consumption of gas sensors with unified MEMS-based circuits [8]. The device integration is traditionally apprehended with a multi-chip method in microcircuits while the sensors are fabricated and designed over distinct chips. The multi-chip integration allows the self-regulating optimization of complementary metal-oxide-semiconductor (CMOS) circuits and MEMS sensors. It offers added flexibility as it minimizes the fabrication steps needed. Though, the additional cost is incurred by intricate packaging [9,10]. This review focuses on MEMS-based sensor platforms, highlighting their fabrication and processing routes, and developments in MEMS/NEMS for gas sensor applications.

The entire review article is organized into various sections as follows. Section 2 describes trends in MEMS gas sensors covering sensor platforms, microheaters, and photonic and fiber optic MEMS. Section 3 overviews the transition of MEMS to NEMS and its applications. Section 4 and 5 cover the materials and manufacturing routes developed for MEMS/NEMS gas sensor platforms. Section 6 discusses the different target gases exposed to the MEMS platforms and their applicability to gas sensors followed by conclusions, challenges, and future perspectives in Section 7.

2. Trends in MEMS gas sensors

Gas sensor platforms are an integral part of gas sensing devices which provide a medium for various gas sensing mechanisms. Therefore, different microfabrication methods used for MEMS fabrication could be shifted towards gas sensors. MEMS technology has gathered solid attention in the area of gas sensing application, such as for the design of sensor platforms, embedding Si cavity for thermal insulation, as well as for deposition of sensing materials [11,12]. One of the prime issues related to gas sensing is to attain a steady operating temperature needed to sustain gas sensing. Various approaches have been attempted to improve the platform design concerning the use of microheaters, manipulation of the conductance and capacitance, isolation of thermal components from the sensing layer, and so on [13].

2.1. MEMS platforms

The sensor platform of a traditional metal oxide semiconductor (MOX)-based gas sensor and a MEMS-based gas sensor platform is presented in Fig. 1 a and b. The sensor platform of the traditional MOX-sensor comprises three core components: the micro-hotplate, gas-sensitive material, and electrodes for signals [14]. In contrast, the MEMS-sensor platform contains an insulation layer, substrate layer, passivation layer, and heater layer. The complete layers are registered as follows: (1) substrate, (2) bottom silicon oxide/nitride layers that insulate the heating element from the substrate, (3) heating element layer and an adhesion layer, if required, (4) top silicon nitride/oxide layer, which assists in utilizing insulation among heater and sensing material and passivation layer to avoid catalytic interaction among target gas and heater material, (5) electrode layer, and (6) gas-sensitive material.

The main role of the MEMS-based gas sensor platform is to increase

the temperature of gas-sensitive material to its optimal working temperature which is the major source of power consumption in gas sensors. The power consumption of the gas sensor is desired to be as minimum as possible, and it depends upon the current and voltage perimeter of the miniaturized gas sensors. MEMS gas sensors are generally utilized to detect volatile or toxic gas in various types of harsh conditions. Therefore, MEMS sensor platforms should be chemically stable at room temperatures and not disintegrate at elevated temperatures. MOX materials are utilized normally in the MEMS-based gas sensor [16,17].

2.2. MEMS-microheaters

The characteristics of a gas sensor are estimated by 3-S parameters, namely, sensor response, selectivity, and stability. In gas sensing, the sensor response is stated as the change in response signal while the response-recovery times are estimated as the time taken to attain 90% variation in the response signal [15]. The ideal MEMS-gas sensor can be recognized as small and portable in size, having a high sensor response, low detection limit (LOD), high selectivity towards various gases, and cross-selectivity. The sensing mechanism for MOX-based gas sensors is related to band-gap energy that leads to a change in electrical resistance. Cho et al. studied a SnO₂-nanotubes deposited MEMS sensor platform with suspended ZnO nanowires (NWs) for enhancing joule heating. The authors found a fast response-recovery time for H₂S gas at room temperature and reduced power consumption [18]. In another report, Zhu et al. described a biomimetic gas sensor based on graphene-Pd nanoparticles for hydrogen detection. The study confirmed a better gas sensor response as compared to chemical vapor deposited (CVD) graphene gas sensors having similar dimensions [19]. The sensor response characteristics of various gas sensors are presented in Table 1.

MEMS technology has enabled the production of different micro/nanosensor platforms offering several benefits in gas sensing fields. The energy consumption could be minimized considerably, specifically by the pulse-mode heating process with a minimum duty ratio [33]. Gas sensor platforms could be reduced in size considerably by complementing them with an external battery that will be valuable to movable gas sensors. The various challenges in microheater performance include high mechanical strength, long term stability and power consumption. Smaller size features of the MEMS platforms could create simple sensor devices which can be accommodated in a small space with numerous gas sensor systems. Temperature distributions throughout the sensing layer must be carefully managed since the sensing characteristics of micro-gas sensors are very temperature sensitive [34]. High mechanical strength is needed for micro-gas sensors during the deposition of sensing film and further processing, as well as for all manufacturing stages involved in fabricating micro-heaters. For practical applications with high sensitivity and a lengthy lifespan, long-term stability is necessary. Reducing heat loss by heat conduction by employing thin beams with a high length-to-width ratio is a well-known strategy for power reduction [35–37]. Nonetheless, inferior mechanical strength is typically the result of the beams' increased length to width ratio. Reducing the active area can also help minimize power consumption by minimizing heat loss through radiation and convection. Sensitivity drops when utilizing a tiny active area since most (bio) chemical sensors

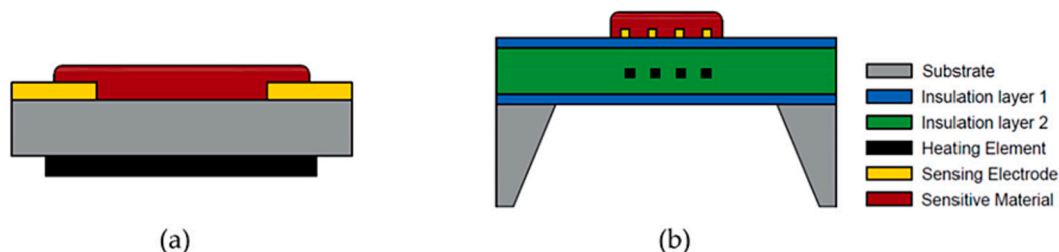


Fig. 1. (a) Sensor platform of traditional MOX-based gas sensor, and (b) MEMS-based gas sensor platform comprising of various elements [14].

Table 1

Sensor response characteristics evaluation of gas sensors. Abbreviations used in Table 1 for sensor response characteristics evaluation of gas sensors are MOX, field-effect transistor (FET), infrared (IR), metal-organic framework (MOF), Zeolitic imidazolate frameworks (ZIF), and room temperature (RT).

Sensing material	Detection principle	Fabrication process	Response time (s)	Detection gas	Operating temperature	Ref.
SnO ₂	MOX	Spin coating	150 s	H ₂ S	200 °C	[18]
Graphene-Pd/Ag	FET	MEMS (lithography)	16 s	H ₂	150 °C	[20]
ZnO NWs	MOX	MEMS (lithography)	50 s	NO	250 °C	[21]
Pt-doped Al ₂ O ₃ /ZnO	MOX	MEMS (lithography)	200 s	Acetylene	120 °C	[22]
Pd-Si	Particle	MEMS (lithography)	12 s	NO ₂ , H ₂	RT (25 °C)	[23]
Pd-Si NM	Diode	MEMS (lithography)	22 s	H ₂	RT (25 °C)	[24]
Absorber material	IR	MEMS (lithography)	5 s	CO ₂	RT (25 °C)	[25]
ZIF	MOF	Solution related	300 s	NO ₂ , H ₂	RT (25 °C)	[26]
Graphene	Band-gap	laser	120 s	H ₂	RT (25 °C)	[19]
YSZ/SnO ₂	MOX	MEMS (lithography)	15 s	SO ₂	400 °C	[27]
Au-In ₂ O ₃	MOX	MEMS (electrospinning)	25 min	Formaldehyde	300 °C	[28]
Au/SnO ₂ :NiO	MOX	MEMS (Self-assembly)	5 min	NO ₂	100 °C	[29]
ZnO-CuO	MOX	MEMS (sputtering)	22 s	acetone	300 °C	[30]
MOF/Co ₃ O ₄ @ZnO	MOX	MEMS (CVD)	3 s	Trimethylamine	250 °C	[31]
SnO ₂ nanosheets	MOX	MEMS Photolithography	–	ethanol	300 °C	[32]

Table 2

Polymer-based gas sensor platform with various sensing materials. Abbreviations used in Table 2 for polymer-based sensor platforms are polypropylene (PP), polyimide (PI), polyethylene terephthalate (PET), polyvinyl acetate (PVA), and nylon.

Sensor platform	Material	Synthesis process	Target species	Ref
PET	ZnO	Hydrothermal	H ₂	[104]
PI	Ga/ZnO	Hydrothermal	H ₂	[105]
PI/PET	Pd/ZnO	Hydrothermal	H ₂	[106]
PET	SnO ₂ /SnS ₂	Hydrothermal	NH ₃	[107]
PET	Polyaniline/ WO ₃	Polymerization	NH ₃	[108]
Cotton fabrics	ZnO	Sol-gel	NH ₃	[109]
PI	Au/In ₂ O ₃ / Polyaniline	Hydrothermal	NH ₃	[110]
PI	CeO ₂ /CuBr	Electron beam evaporation	NH ₃	[111]
PI	Polyaniline/ CeO ₂	Self-assembly	NH ₃	[112]
PP	ZnO _{1-x}	Suspension flame spraying	NO ₂	[113]
PI/PET	WO ₃ /MWCNT/ rGO	Hydrothermal	NO ₂	[114]
PP	SWNT/Fe ₂ O ₃	CVD	NO ₂	[115]
PET	rGO/WO ₃	Hydrothermal	Isopropanol	[116]
PI	Ag/ZnO	Hydrothermal	C ₂ H ₂	[117]
Nylon	ZnO	Hydrothermal	H ₂	[118]
PVA	In ₂ O ₃	Hydrothermal	Ethanol	[119]

have bigger active areas with superior detecting mechanisms. This conundrum forces researchers to strike a compromise between mechanical strength, sensitivity, and power consumption.

Previous authors studied 3D micro-heater that features a Pt heating resistor inserted in a concave active area. In comparison to existing 2D micro-heaters, the 3D micro-heater demonstrated reduced power per active area by reducing heat loss through thermal convection and radiation. It is possible to create a micro-heater with a high active area and low power consumption using such an innovative structure [38]. Recently, pulse driven preheating of SnO₂ nanoparticles sensor was carried out to enhance its sensing capabilities against volatile organic compounds. The pulse heating included double-pulse consisting of brief

preheating cycle at a high temperature followed by a cooling cycle followed by a measurement cycle. Such an operating profile Because of this operating profile resulted in improved O²⁻ ions adsorption and ethanol based adsorption for efficient gas sensing [39].

2.3. MEMS photonic crystals and fiber optics

It is a noteworthy point to say that these MEMS/NEMS gas sensors are not used only for heating but also used in other applications. Several MEMS gas sensing platform variations have been commercialized in a wide range of applications. The examples include health care diagnostics [8,9], food quality monitoring [10,11], agriculture [13], and pipeline leak detection [12]. The optical gas sensor such as MEMS photonic crystal cavity and fiber optic sensors have played a great role in gas sensing. Photonic crystal cavity has periodicity in the dielectric constant as proposed by Yablonovitch and John in 1987 [40,41]. Photonic crystals can control light wavelengths and produce unique effects that are impossible with traditional optics. Previous research activities have seen several 2D photonic crystal cavity gas sensors (Fig. 2a) due to a higher quality factor (Q) than other configurations [42].

The mechanism of the photonic crystal gas sensor is described by Bragg's law.

$$m\lambda = 2\mu d \cdot \sin\theta.$$

where m is the diffraction order, λ is the wavelength of light, μ is the effective refractive index of the periodic structure, d is the interplanar spacing, and θ is the glancing angle, respectively. A change in the refractive index and the lattice distance will affect the diffraction wavelength and hence the detection of gas is made feasible [42]. Photonic crystals can be produced by MEMS lithographic techniques, e.g., electron beam lithography [43], self-assembly, or CVD [44,45]. The dimensions of the photonic crystal cavity can be controlled accurately using MEMS micromachining techniques.

In comparison, fiber optic sensors have attracted enough research interest owing to their ability to monitor harmful gases. Fiber optic sensors consist of a sensing element, core, and a clad, as shown in Fig. 2b. If there is a change in refractive indices of the outer layer and inner core of fiber (outer layer < inner core), total internal reflection occurs, and light propagates in the core [46]. Conversely, if refractive indices values of clad and core are too close, the light will be propagated

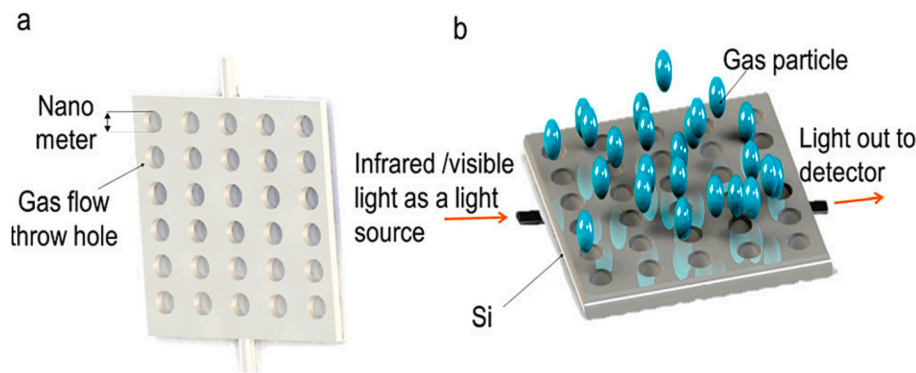


Fig. 2. (a) Schematic view and (b) mechanism of a photonic crystal gas sensor.

and penetrate the clad region. The optical properties of the core and clad layer will be changed in the presence of target gases which will cause a change in the refractive index of the sensing layer [46]. Different types of MEMS-based fiber optic sensors include Fabry-Perot [47], photonic crystals [48], evanescent waves [49], surface plasma resonance [50], etc.

Other MEMS gas sensors include acoustic wave gas sensors which utilize mechanical, or acoustic, waves for gas sensing [51]. The acoustic gas sensors have better gas detection performance due to the ensuing interactions which can be easily identified at lower ppm levels [52]. However, the limited selectivity of the acoustic sensors is related to the sensing materials used. Examples of acoustic sensors include quartz crystal micro-balance and surface acoustic wave sensors.

3. Evolution of MEMS to NEMS

Repeated heating and cooling of the bulky MEMS platforms have raised concern over the development of innovative energy-saving approaches in the past [53]. Possible gas response signals at various working temperatures would be attained in a few seconds. The relation between gas response and working temperatures would be a beneficial means to detect target gases [54,55]. As stated earlier, gas sensors are anticipated to remain revolutionized by the usage of nanosensor platforms based on NEMS. Though, there is a need to stand clear before the developed gas sensors are commercialized. One of the methods is to follow nanofabrication methods to deposit the sensing layer homogeneously on nanosensor platforms. Moreover, micro/nano-characterization techniques must also be well-known [56]. The most appropriate way for the fabrication of the MOX sensor platform is the

integration of MEMS sensor platforms with gas-detecting nano-structured materials. This method guarantees better 3S parameters (sensor response, selectivity, and stability) which are typical of nano-structures synthesized by various approaches [57].

The shrinking of MEMS-based gas sensors reduced to submicron or lesser drives to the area of nanotechnology that was profoundly endorsed in the past decade [58,59]. In general, the integration of microelectronics and nanotechnology is known as the field of NEMS [60,61]. NEMS appeared in the early 2000s. Unlike MEMS, NEMS is an emerging technology. Extremely small features improve the reaction kinetics and are highly sensitive to a number of stimuli. Fig. 3 shows the typical bulky mechanical structures of micro-accelerometers present in airbags to modern nanostructures whose electro-mechanical properties can be profoundly modified by their quantum size effects. The extreme sensing performance of nanostructured sensors opens the way to diverse applications of NEMS sensing platforms in bio-analyses that cannot be achieved by their big brothers, MEMS [62], force sensors [63,64], and ultrasensitive mass sensors [65–67].

On the contrary, MEMS technology is frequently relied on top-down fabrication methods, while NEMS is associated with mostly bottom-up methods to create important materials and device platforms such as nanotubes, NWs, and two-dimensional (2D) nanostructures and carbon nanomaterials. The technologies-based NEMS are in the initial phase of growth. However, research is swiftly gaining momentum and an increasing number of NEMS-based gas sensors are being reported in the literature [69,70]. The important disadvantages of MEMS over NEMS technology are the extremely high cost of research and development, expensive fabrication techniques, and scaling issues for any MEMS design or device. In addition, the setup cost for cleanroom facilities can

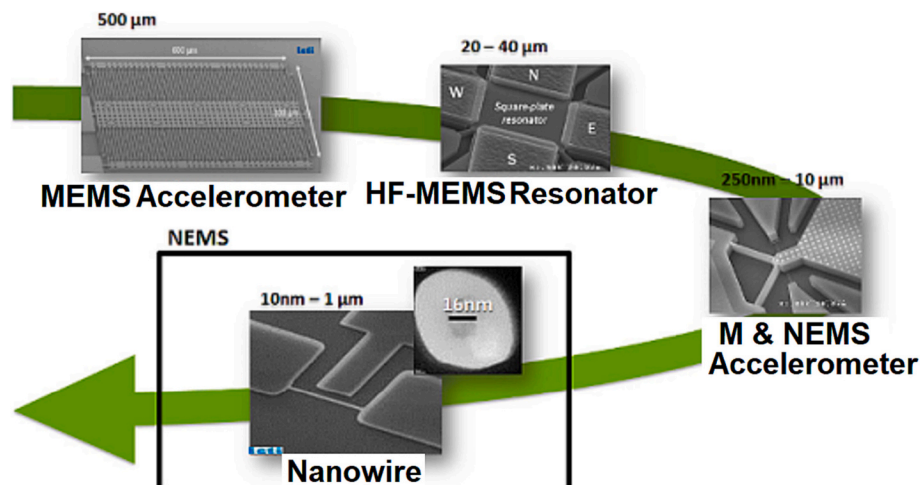


Fig. 3. Schematic of the NEMS sensor platform for gas and chemical detection [68].

be very high for even low quantities. NEMS has advantages of high efficiency, reduced power consumption, and miniaturization down to 100 nm. Small mass and size provide additional attributes like the potential for new nanoscale applications and measurements.

Nanoimprint lithography can be used to fabricate polymer-sensitive sensor platforms for the detection of air-borne vapors such as ethanol, acetone, and thiols (Fig. 3). Lately, a multi-gas examination scheme relied on NEMS was capable of sensing gas at low concentrations. Because of minute mass and high resonance frequency, NEMS-based gas sensors are capable of improved gas sensing. These NEMS-based gas sensors have been applied in industrial organizations for real-time analysis of gas mixtures [70].

4. Materials for MEMS/NEMS platforms

Several microelectronic devices use semiconducting materials for MEMS such as silicon. As such, Si is the most widely used substrate for MEMS/NEMS fabrication due to its dimensional stability, thermal stability, and compatibility with widely adopted lithographic fabrication technologies and packaging techniques. There are other materials also used for MEMS platforms such as ceramics, glass, polymers, etc.

4.1. Silicon

Silicon (Si) is a primary material of choice for MEMS-based gas sensors because of its attractive semiconducting features required for MEMS design and fabrication [71,72]. The well-known micromachining procedures with additive methods make the design and production of Si-MEMS easy and cost-effective. The process flow diagram of silicon micromachining is shown in Fig. 4a.

(a) diagram, and (c) photographic image of MEMS-based gas sensor [30].

The diagram and photographic image of the gas sensor are shown in Fig. 4b-c. Si-MEMS devices might have materials that are well-suited to Si including oxides, nitrides, carbides, and metals, for instance, W, Al, Cu, and polymers for example polyimide. Apart from benefits from

MEMS technology, it does not allow heating of sensing material at temperatures $>350\text{--}400\text{ }^{\circ}\text{C}$ in operation and does not allow technical heating at high temperatures essential for the maintenance of characteristics of MOX sensing material ($600\text{--}700\text{ }^{\circ}\text{C}$) [73–75].

Present silicon MEMS technology in mass production is unable to adequately heat the MOX sensing layer ($700\text{--}800\text{ }^{\circ}\text{C}$) or heat the sensing layer at $300\text{--}350\text{ }^{\circ}\text{C}$ during operation. With the exception of platinum, the long-term stability of the heater presents a challenge at high temperatures in both oxidative and reducing environments. Because of its low adherence, platinum deposition and stability on SiO_2 substrate present some challenges. Ti was employed as an adhesive layer for Pt deposition by the authors [76]. They discovered that the Pt layer exfoliates from the surface after 30 min of heating at $500\text{ }^{\circ}\text{C}$. The specifics of this issue were covered in [77]. To increase adhesion, some people employed an adhesive film made of a combination of silicon oxide and platinum nanocrystals [78].

4.2. Alumina

Perfect platinum adherence to alumina, even after high-temperature annealing, is a significant benefit of using alumina as a substrate rather than silicon oxide or nitride material for silicon-based microhotplates. Since adhesion is the outcome of the interaction of two interface materials, the substrate's function in platinum adhesion is obviously highly crucial. The first effort to design and fabricate a ceramic-based microheater is made by alumina. The benefit of using alumina as a substrate over silicon nitride or oxides micro hotplates relies upon the excellent adhesion of platinum (Pt) to alumina ceramics at elevated temperatures [79]. The micro-hotplate comprises of hot portion with $20\text{ }\mu\text{m}$ ceramic legs and a heater for the sensing material. Ceramics-based gas sensors face demerits such as high-power consumption due to the high-heating power of gas sensors. Ceramic sensor platforms involve multilayer ceramics, probably to evade the method of etching of ceramic-based sensor platforms, for instance, the stack of low-temperatures co-fired ceramics (LTCC) sheets [80,81]. The possible methods to reduce power consumption are the usage of the thin-glass film with a similar thermal-

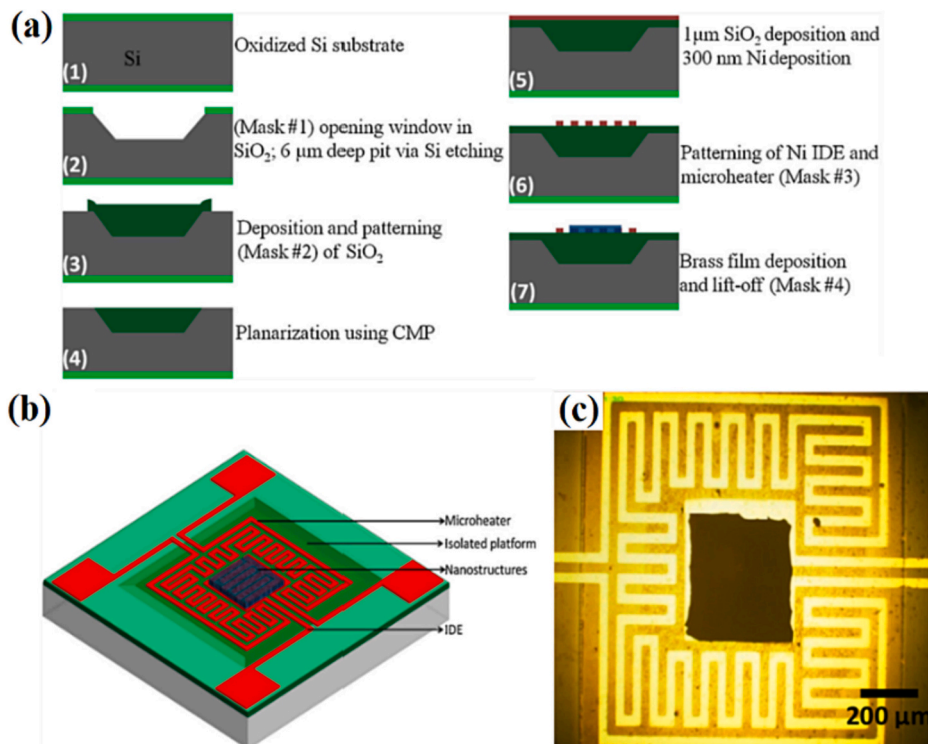


Fig. 4. (a) Schematic process flow for Si-based gas sensor platform fabrication, (b).

expansion coefficient matching with LTCC. Fig. 5 demonstrates the design of the ceramic-based sensor. The ceramic MEMS presented in the picture is formed by utilizing an alumina thin-film adhered by sealing glass on an alumina sensor platform with a cut-out hole.

Several microheater designs have been studied in the past to reduce power consumption and increased energy saving [84]. Previous reports have shown promising reductions in power consumption however microheater gas sensors remain unsatisfactory at the system level. The temperature distribution across the microheater during sensing remains a challenge that reduces the sensitivity and reliability of the device. Some improvements have been made further in microheater gas sensors such as modification of the sensing layer via NW [15,16] or optical sensors [17]. However, MEMS-based microheaters are still in the picture.

4.3. Thin ceramic films and membranes

The formation of thin alumina films (TAF) is the most popular method to improve energy saving in ceramic sensor platforms. The membrane could be formed through electrolytic oxidation of light metals such as Al, Ti, Mg, etc. These TAF-based gas sensor platforms have been utilized for gas sensing applications. The electrolytic oxidation of metals occurs at high temperatures and potentials in plasma electrolytic oxidation over anodizing chemical method [85]. After oxidizing the metals, TAF is fabricated from the surface via etching. TAF-based MEMS gas sensors could resist high temperatures up to 550 °C. The power consumption of TAF based MEMS gas sensor platform is equivalent to the results obtained from the Si-based gas sensor platform [86]. For instance, MiCS5524 CO gas sensors have a power consumption of 70–85 mW at operating temperature that is equivalent to around 300 °C. Despite significant results attained with TAF membranes

created by electrolytic oxidation of Al, high porosity, and surface defects of alumina restricts wire bonding of Pt on the MEMS-based sensor platform [87]. One more shortcoming of TAF is the roughness of the surface, which requires a fairly thick Pt heater (~1 μm) through the magnetron sputtering method. Furthermore, porous membranes formed via electrolytic oxidation of Al are sensitive to mechanical and thermal damage.

The MEMS-based gas sensor platform on anodic alumina was presented by D. Routkevich in 2001. A significant benefit of this method is the mask-less technology of micro-hotplate formation. Pt was coated on an alumina substrate, and a horse-shoe-shaped microheater was made by laser cutting Pt with alumina substrate [88]. This micro-heater sensor platform could be simply heated to 700 °C. Temperature homogeneity for this particular sensor platform is comparatively consistent over the portion shielded via a sensing material. The foremost hindrance of this micro-heater sensor platform is the fragility of the chip and difficulties with the packaging of large and thin-area platforms. So, the opinion of simple packaging was reinstated to fix the membrane in a similar way to the Si-based gas sensor platform [89,90]. Thin-membrane created by nanoporous alumina was used in a ceramic MEMS-based gas sensor platform, well-known as anodic aluminum oxide (AAO, Fig. 6a-d).

A major problem in the fabrication of AAO membranes is mechanical disintegration that results in the distortion of primarily plane AAO membranes through high-temperature annealing beyond ~550 °C. This hindrance restricts the applications of AAO membrane in gas sensing applications annealed around ~600–800 °C [92]. Also, high-temperature material, for instance, gallium oxide (Ga₂O₃), is utilized as sensing material with working temperatures above 550 °C. A significant benefit of the MEMS-based sensor platform made by AAO membrane as compared to the Si MEMS-based sensor platform is the possibility of laser-machining on alumina due to the stress-free alumina

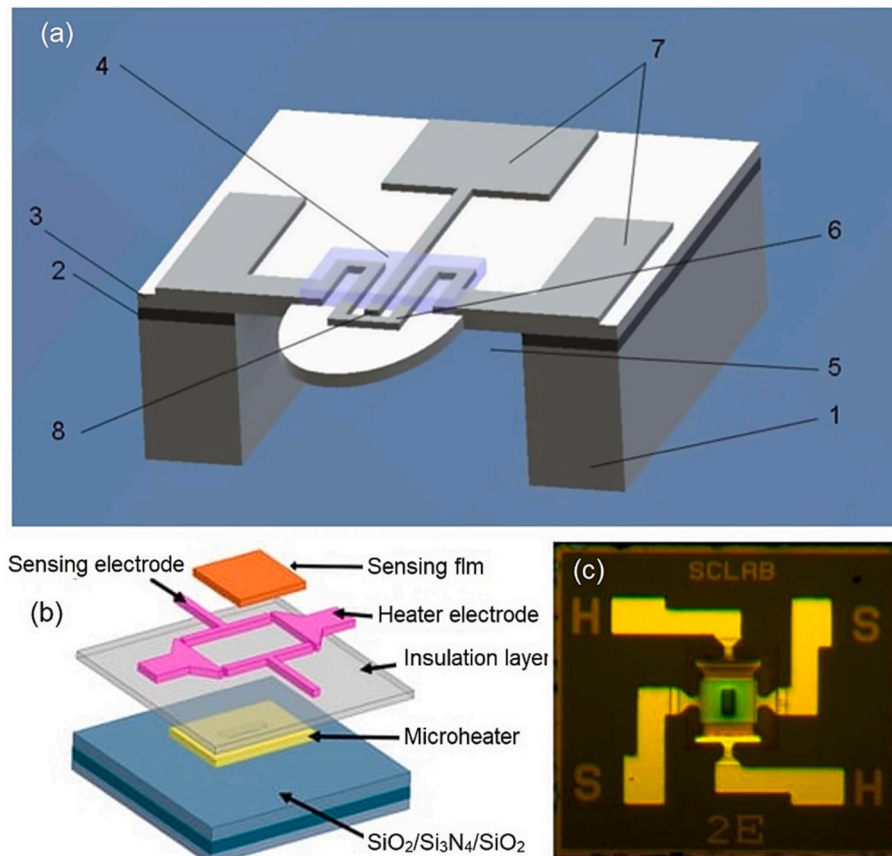


Fig. 5. (a) Design of ceramic MEMS sensor 1) ceramic platform; 2) adhesive layer; 3) thin-film ceramics membrane; 4) sensing thin-film; 5) laser penetrated hole; 6) Pt micro-heater; 7) contact pad; 8) sensing electrode [82]. (b) MEMS microheater and (c) real image of microheater [83].

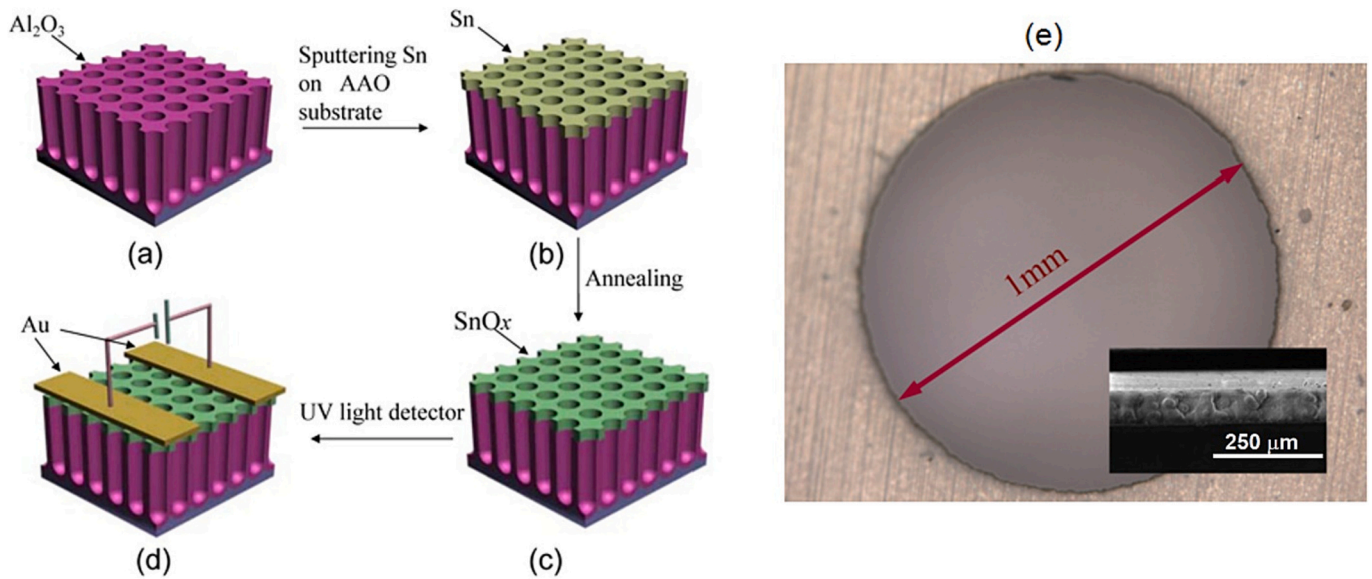


Fig. 6. Diagram of fabrication procedure of SnO₂ nano-pore thin-film. (a) AAO pattern; (b) top-view of SnO₂ nano-pores; (c) annealing at various temperature; (d) SnO₂ nano-pore thin-film based UV photo-detector [91], and (e) 1 mm in diameter hole drilled by laser in 20-μm alumina thick-film and SEM image of edges of laser-cut [40].

thin films in contrast to Si- membranes [93]. A similar case of, a 1 mm laser-drilled hole, is shown in Fig. 6e. The cutting procedure does not result in the creation of cracks in membranes as presented via the scanning electron micrograph (SEM) in the inset of Fig. 6e. Therefore, the laser could be useful for the creation of holes, and added essentials of MEMS capable of progress process of chemical sensors related to alumina membranes [40].

4.4. Zirconia and borosilicate glass ceramics

The core benefit of using ZrO₂ ceramics in comparison to other ceramic materials is due to its thermal conductivity which is ten times lower than that of Al₂O₃. Thus, the MEMS-based gas sensor platform created by zirconia ceramics would acquire significantly lesser power as

compared gas sensor platform created by alumina with a similar thickness [94,95]. Also, as compared to the Si-based gas sensor platform zirconia-based gas sensor platform requires less power consumption for gas sensor applications [96].

The key motive for the claim of thin-film borosilicate glass as a substrate for gas sensors is the fabrication through facile low-cost equipment [97]. A significant advantage of using a thin-film borosilicate glass sensor platform is its attractive thermal expansion coefficient which is almost similar to LTCC and Si [98,99]. Therefore, a suitable MEMS-based sensor platform can be fabricated by positioning a glass cantilever on a ceramic platform. Fig. 7a shows the fabrication of a glass micro-heater utilizing a laser pattern for the heater. Later, laser beam carving of Pt micro-hotplate, a similar laser beam was utilized for cutting of platform and piercing holes utilized for soldering platform to TO-

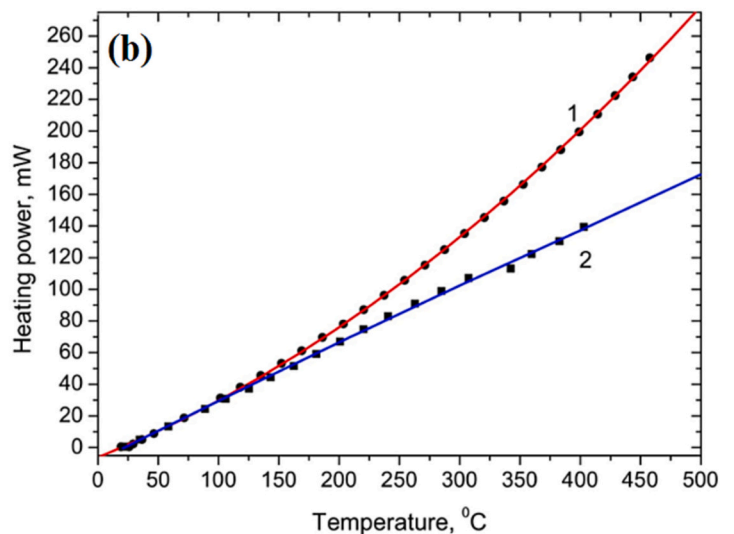
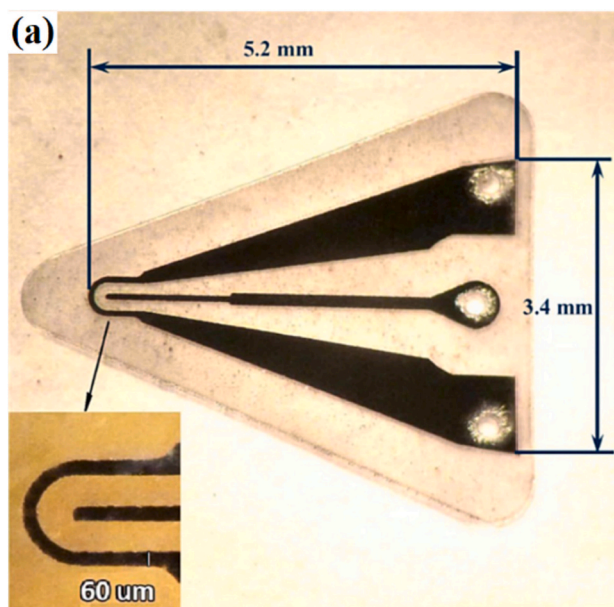


Fig. 7. (a) Micro-heater on 30-μm thick-film borosilicate glass as a sensor platform. Pt micro-heater is fabricated via laser ablation, (b) Power-consumption of micro-heater: (1) whole-membrane with micro-heater positioned in middle; (2) triangle profile cantilever with a micro-heater positioned at the tip of cantilever [40].

8 sensor package. The thermal characteristics of the micro-heater created by 30- μm borosilicate are shown in Fig. 7b. The power profile changes according to the positioning of the micro heater which can be tuned effectively.

4.5. Polymers

Polymers are utilized for fabrication in wearable gas sensor applications that have very low conductivities ($<10^{-6} \text{ Scm}^{-1}$). The core monomers of polymer comprise alternate single/double bonds [100]. Polymers have been extensively explored for development as a flexible substrate to achieve flexibility and improved sensing characteristics at RT. Poly(3,4-ethylene dioxythiophene) (PEDOT), polypyrrole, polyaniline (PANI), and polythiophene (Pth) are the foremost polymers utilized in gas sensors [101,102]. Seekaew et al. studied an ammonia gas sensor based on PEDOT/PSS sensing material and the sensor showed a 10% sensor response towards 100ppm ammonia. The sensor response of PANI-based nanoparticles on PET substrate was examined and the sensor showed improved sensor response as compared to the Si-based substrate [103].

Polymers have attracted progressive significance in the field of MEMS. It would not ever substitute conventional materials such as Si in mass MEMS production, their assets lie in their possible benefits in various fields such as rapid prototyping, biological systems, and robust operations [119]. The precise practical tests in microfabrication, include patterning, deposition, and bonding with polymers, along with typical demonstrations of their applications that include gas sensors, and microfluidics [120]. Thuau et al. studied a series of electromechanical transduction systems for usage in polymer-based MEMS sensors [101]. The main devices and materials comprise nanocomposites based on carbon nanotubes (CNTs), polymer sensors created by (Polyvinylidene fluoride (PVDF) -trifluoroethylene (PVDF-TrFE). These polymers are mainly designed for sensor platforms and detecting applications and prove that nanocomposite and polymer MEMS could be fabricated and combined for complex purposes.

Polymer MEMS with three-dimensional (3D) printing machinery is confirmed by Kundu et al. and Lamperska et al. [121,122]. They utilized two-photon lithography to make micro-dumbbell assemblies that could be manipulated by optical tweezers. An example of the fabrication of polymer-based gas sensors with interdigitated electrodes (1 mm spacing) is used for the inkjet printing of the polymer substrate (see Fig. 8 a–b). The gas sensor with graphene@PEDOT/PSS is shown in Fig. 8 c–d. The thicknesses of graphene–PEDOT:PSS sensing thin-film was around 407 nm [123].

When compared to the polymers, the Si wafer's microheater offers superior thermal uniformity. Moreover, because of their flexibility and deformability, microheaters with PDMS substrates can be used on non-flat surfaces and require a lot of power to achieve the same maximum temperature on Si wafer [124]. Silica glass has higher electrical resistivity and lower thermal conductivity than silicon, they are used as base substrates that result in heat confinement and low power usage [125,126]. The comparison of several substrates indicates that the microheater on glass reached about 300 °C, while the microheater on silicon and alumina only produced very little heat at 320 mW power [127]. According to all of these studies, the substrate plays a crucial part in maintaining the proper temperature by preventing heat loss.

5. MEMS fabrication techniques

As already discussed, MEMS fabrication techniques are crucial for MEMS-based gas sensor platforms. Various technologies used for MEMS fabrication involve ion implantation, oxidation, metal sputtering, CVD, and diffusion methods [128–130]. Lithography is an important method for MEMS/NEMS fabrication. The progress of this technology is crucial to minimizing the drawbacks of MEMS/NEMS fabrication. Aiming the innovative fabrication methods, innovative materials, and innovative structures, would attract future MEMS/NEMS gas sensor platforms that are practical and effective in academic and industrial zones [131–133]. The lithography can be used to pattern materials and create structures with controlled porosity. This can significantly increase the effective

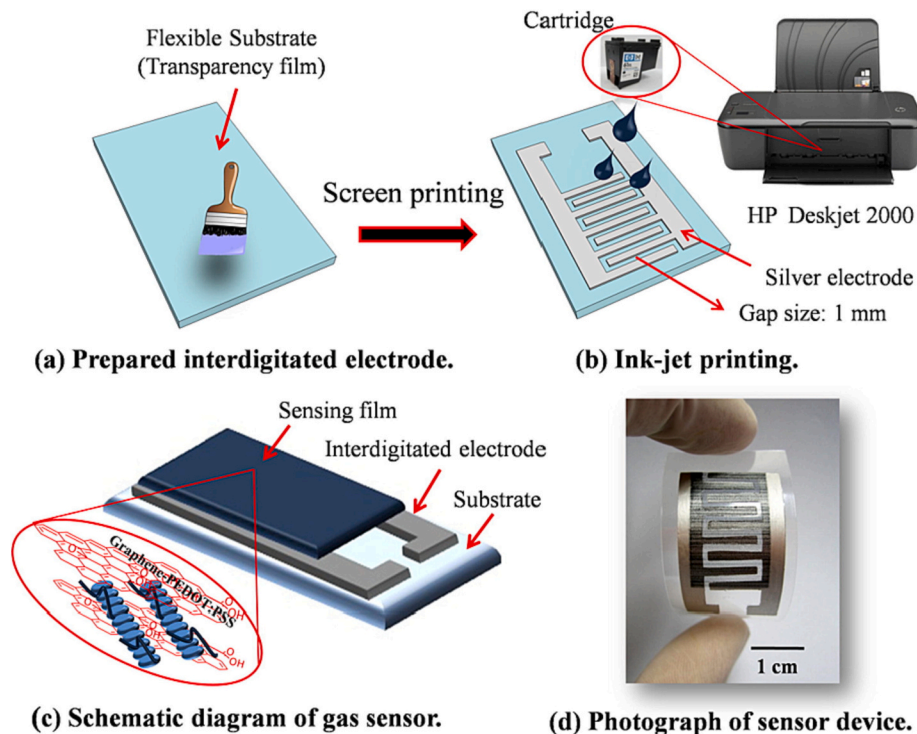


Fig. 8. Schematic for gas sensor fabrication procedure. (a) prepared interdigitated electrode, (b) ink-jet printing, (c) schematic diagram of a gas sensor, and (d) photograph of a sensor device [123].

surface area and tune the morphology of the sensing material. This controlled porosity can influence gas adsorption and desorption kinetics, impacting the gas response. Therefore, in this section, we discuss various lithographic fabrication methods used for MEMS sensor platforms.

5.1. Edge lithography

Edge-lithography is another term for lithography which practices edge portions of traditional nano/micro-sized assemblies. High-resolution assemblies fabricated by edge-lithography could be simply created by narrow edges of traditional nano or micro-sized pre-assemblies which are simple to develop. The notion of edge lithography is presented by edge arrays through light interference at the edges portion of phase shift mask assemblies, which merely lessens nano-pattern size [134–137].

These edge-lithography approaches have been used in an extensive variety of functions that include a gas sensor platform, transparent electrodes, and optical devices. Edge lithography has numerous benefits; easy to lessen magnitudes, for instance, dimensions and pitch via parting individually sides of preassembly [138–140]. Moreover, this technique does not involve intricate methods and exclusive equipment. Also, numerous applications for improving characteristics utilizing high-resolution edge nano assemblies could offer a high surface-to-volume ratio. Edge lithography could be characterized by a technique utilizing the edge part (Fig. 9). We would define structures and principles of four characteristic edge lithography approaches that include spacer lithography, phase-shift lithography, edge spreading lithography, and modified capillary force lithography.

5.2. Phase shift lithography

Phase-shift lithography is planned to improve the resolution of lithography by utilizing a phase shift mask on the way to produce a phase shift by employing groove assemblies or alternative material deposition. To lessen magnitudes of lithography, phase-shift lithography

utilizes interference phenomena of light at the edges area of phase shift mask assembly and, thus, creates assemblies smaller than the wavelength of light [138–140]. Though procedures similar to outdated lithography, different traditional photomask with impervious assemblies, photomask utilized in phase-shift lithography is translucent incomplete areas. Photomask in phase-shift lithography has micro/nano-sized structures that originate from phase shift [141,142].

Hence, an important aspect of phase-shift lithography is the relation between incident light wavelength and the magnitude of the phase shift mask assembly. Phase shift lithography is a facile technique to attain nano-patterns at 20–90 nm dimensions by the usage of phase shift photomask in traditional lithography methods. Utilizing a phase-shift mask of several dimensions, numerous high-resolution assemblies could be created. To attain smaller nano-pattern through phase shift lithography, integration with further lithography approaches for instance post-etching method is essential [143,144].

Fig. 10 shows the exposure phase shift lithography for positioning NWs. With this method, numerous nanostructures could be fabricated. For instance, Fig. 10 (b) Si-based nanoneedles, (c) fence-like Si NW arrays in box-like shape overgrown by ZnO demonstrating nanocontainers, and (d) an array of NWs prepared by phase shift lithography assist [145].

5.3. Spacer lithography

Spacer lithography has been utilized mainly to lessen the dimensions of nano-patterns by employing side-edge of prevailing nano-pattern [146–150]. Also known as spacer-defined double patterning (SDDP) or self-aligned double patterning (SADP) as it involves a multi-step patterning procedure [151,152]. Spacer lithography uses film coated on side-edges nano-size assemblies as one assembly [153]. A pre-assembly for coating spacer material is fabricated by numerous lithography approaches for instance nano-imprint lithography and photolithography. The spacer material is coated on pre-assembly. A homogeneous deposition is significant as it deposits the side edge of the pre-assembly through the coating. To entirely shelter side-edges of pre-

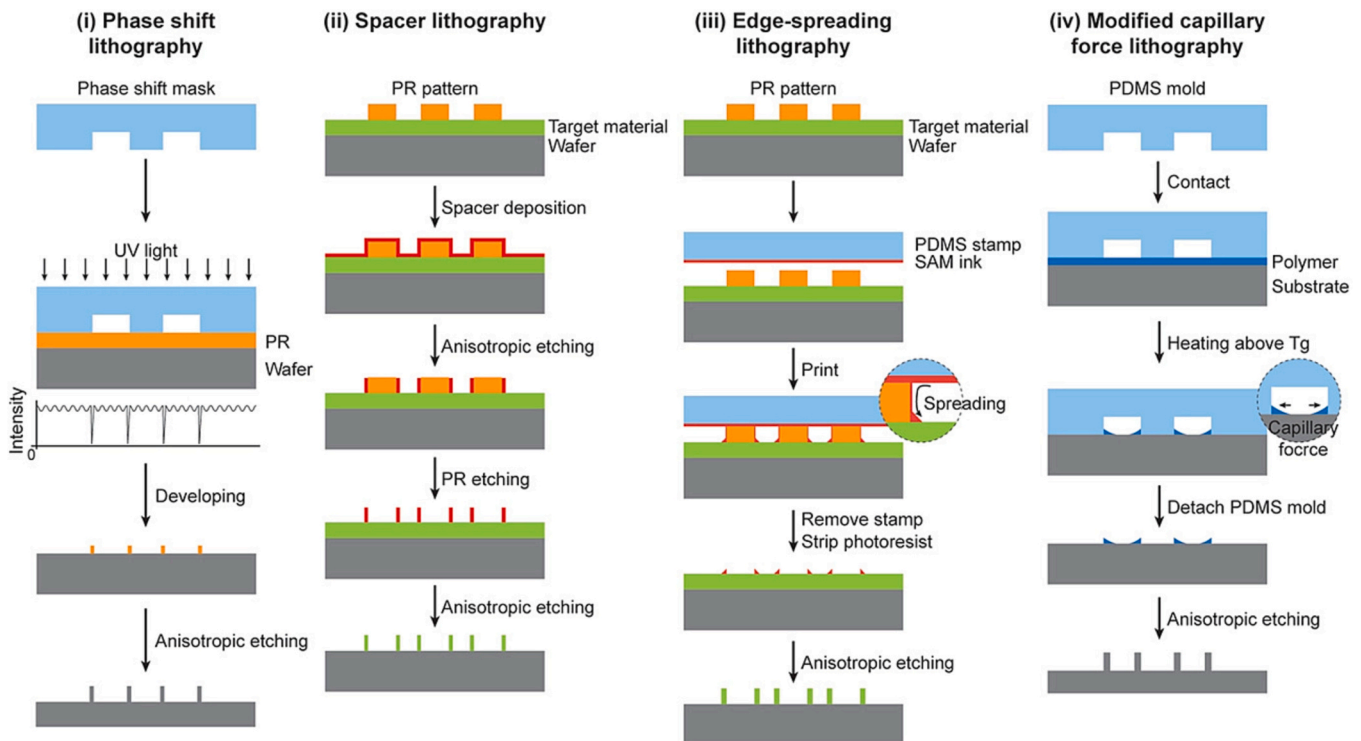


Fig. 9. Four various edge-lithography methods based on approaches for using edges. Edge-lithography could be characterized contingent on the technique for utilizing the edges. i) Phase-shift lithography, ii) spacer lithography, iii) edge spreading lithography, and iv) modified capillary-force lithography [137].

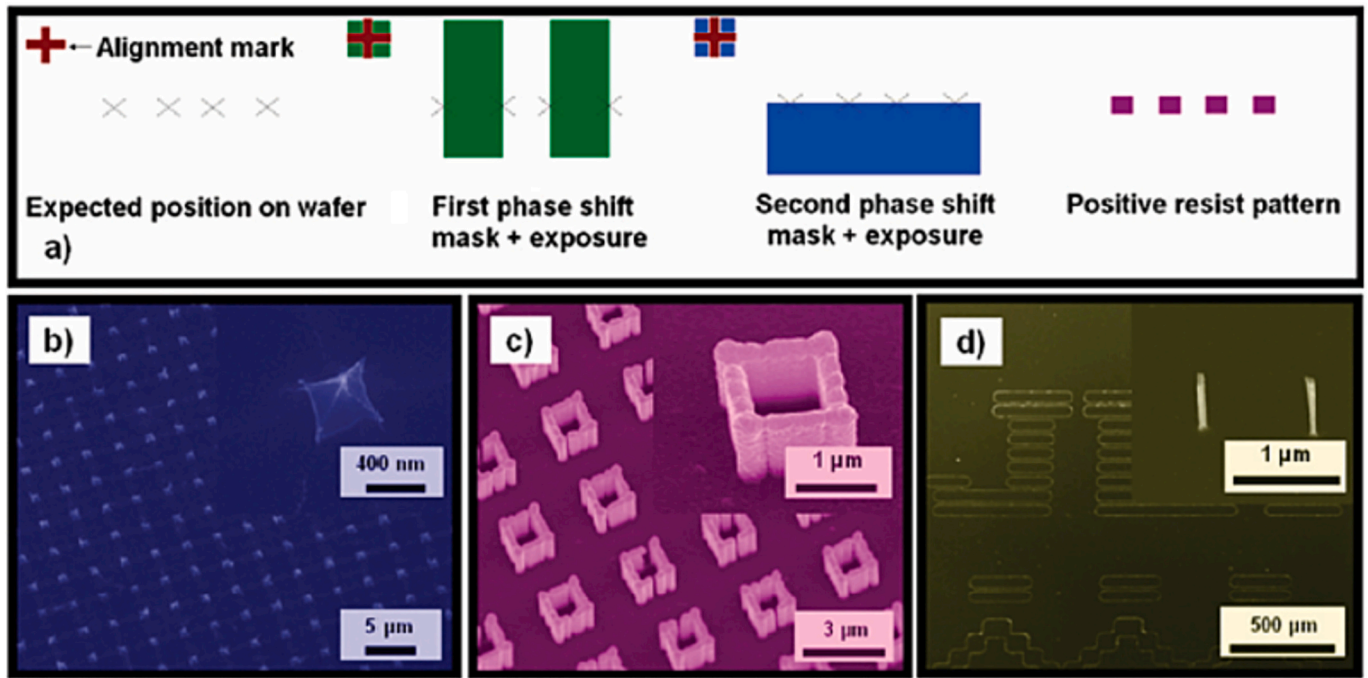


Fig. 10. (a) Two-step exposure phase shift lithography for placing NWs. Numerous nanostructures could be fabricated with this procedure. For instance (b) Si-based nanoneedles, (c) fencelike Si NW arrays in boxlike shape overgrown by ZnO demonstrating nanocontainers, and (d) an array of NWs prepared by phase shift lithography assist [145].

assembly, vapor deposition are utilized [154–157]. Reactive ion etching (RIE) is utilized to etch spacer material parting only thin film on pre-assembly side edges.

Lastly, the selective elimination of pre-assembly materials withdraws thin spacer materials on pre-assembly side-edges. Spacer materials are primarily utilized as a mask to transfer spacer assembly to material deposited underneath, then spacer assembly to the material beneath, spacer could be entirely detached to attain high-resolution assembly over massive part. Demami et al. fabricated polysilicon NWs by the side-wall spacer Lithography technique. Fig. 11 shows the fabrication of polysilicon NWs by the side-wall spacer-lithography method. The cross-section SEM image shows the 50-nm polysilicon NWs and 10-μm polysilicon NW-based resistors [158].

5.4. Edge spreading lithography

Edge spreading lithography (ESL) creates assemblies on the edges of assemblies utilizing the fluidity of the target material. ESL is planned to pattern self-assembly monolayer (SAM) for instance alkanethiol and was originally recognized via Xia’s research group [159]. Materials of SAM on the upper layer are stimulated by nanostructures to the substrate beneath and placid at the edge of the structure. Therefore, structure facilitates the drive of alkanethiols particles and regulates the shape of SAM assembly [160–162]. SAM materials are created in a pattern on the outer edges of the photo-resist assembly. After that, a high-resolution assembly could be attained by eliminating photo-resist and etch gold (Au) through SAM assembly employing a mask. ESL technique could be utilized for numerous assemblies likewise as a photo-resist pattern.

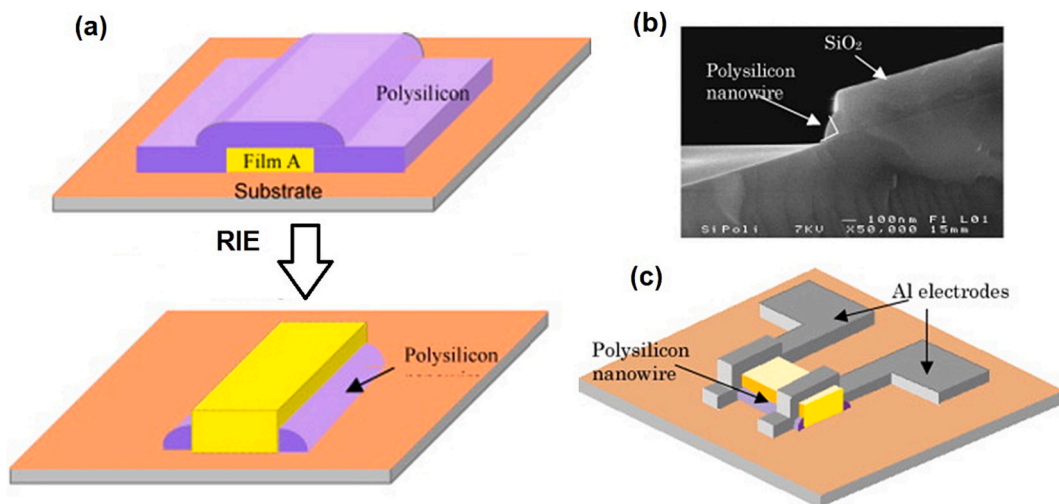


Fig. 11. (a) Fabrication of polysilicon NWs by side-wall spacer-lithography method. (b) SEM photo 50-nm polysilicon NWs cross-section view. (c) Spacer technique 10-μm polysilicon NWs based resistors [158].

5.5. Modified capillary lithography

Capillary-force lithography (CFL) is a technique for the assembly of a broader diversity of fluidity material. CFL practices mold-stamp to make polymers assembly. In CFL, polymer melts and fills the voids among molds and polymers. As the stamp is detached from the substrate, polymer assembly is formed [163,164]. The CFL technique is based on capillary forces, dissimilar height assemblies could be formed at the edge of the pattern liable on the number of polymers and profile of assembly. Utilizing high-resolution polymers assembly utilizing a mask, the material is etched to attain high-resolution assembly with chosen material [165–167]. The profile and size of the assembly could be accustomed following the thickness of deposited polymer materials, etching period, the shape of the stamp, and other aspects. Besides, edge lithography utilizing ESL and CFL, numerous methods relied on dewetting phenomena utilizing fluidity of assembly material, and edge transfer technique utilizing the stamping method has been established [168–170].

Assemblies formed through SSL and edge approaches have a high surface-to-volume ratio that could be a benefit for displaying high sensor response in numerous gas sensors. Thus, the structure created through SSL and edge has been extensively utilized to increase sensor response. The usage of nanostructures or assemblies in gas sensor platforms frequently enhances the performance of conventional thin-film sensor platforms [171]. Edge lithography is an appropriate method for producing high-resolution sensor platforms and displays improved sensor response with a high surface-to-volume ratio in comparison to traditional thin-film sensor platforms. Thus, high-resolution polymer or MOX assemblies are fabricated by edge lithography to display enhanced sensor response outcomes for target gases (Fig. 12 a) [172,173]. Also, nano-assemblies formed thru by spacer lithography are well suitable for the gas sensor that attains a high surface-to-volume ratio due to its high aspect ratio. The spacer lithography technique has the benefit of being a gas sensor platform that could utilize several sensing materials.

For hydrogen (H_2) gas sensors, research is concentrated mainly on Pt

and Pd alloys. The Pt nanostructures-based H_2 sensor was formed by SSL that showed exceptional sensor response, low LOD around 1 ppm, and excellent recovery performance at room temperature (Fig. 12 b) [166–168]. The ultra-small grain size and thin interface gap and surface electrons scattering principles to instantaneously functional towards sole Pd channel, thus persuading dual switching sensor response towards H_2 (Fig. 12 c) [176,177]. Lately, H_2 gas sensors utilizing Pd-created multi-component nano-assemblies have been developed (Fig. 12 d) [108]. Depending on present research using sole particle Pt and Pd; Penner et al. [178] studied numerous binary structures to advance sensor response. When Au or Pt are varied in Pd through spacer lithography, the reaction rate was enhanced [178,179]. Pd–Au binary structures exhibited a response time of 2 s for 1% H_2 gas which is the fastest response rate stated to date (Fig. 12 e).

6. Target gases and MEMS sensors

MOX-based sensors have been used widely to detect various toxic gases such as HCHO, C_6H_6 , and naphthalene, C_2H_5OH . The concentration of these gases ranges from ppm to sub-ppb level detections [180]. For high-level ppb detection, MOX gas sensors are designed to operate at elevated temperatures known as temperature cycled operation to improve sensitivity and selectivity. In temperature cycle operation, the microheater unit of the sensor is exposed periodically to a different set of temperatures that lead to different interaction statistics of sensitive layers and analytes [180,181].

Recent research has shown that the selectivity of the sensor devices can also be increased by utilizing the physisorption effect. The sensitivity and selectivity is affected by the operating temperature of the obtained structures. The effective methods used to tune the sensing properties of the obtained materials to provide different response spectra suitable for exploitation in an electronic nose instrument include the proper choice of metal oxide, the ability to control the physical-chemical properties of these materials, i.e., their stoichiometry, porosity, grain size and shape, as well as the proper addition of dopants

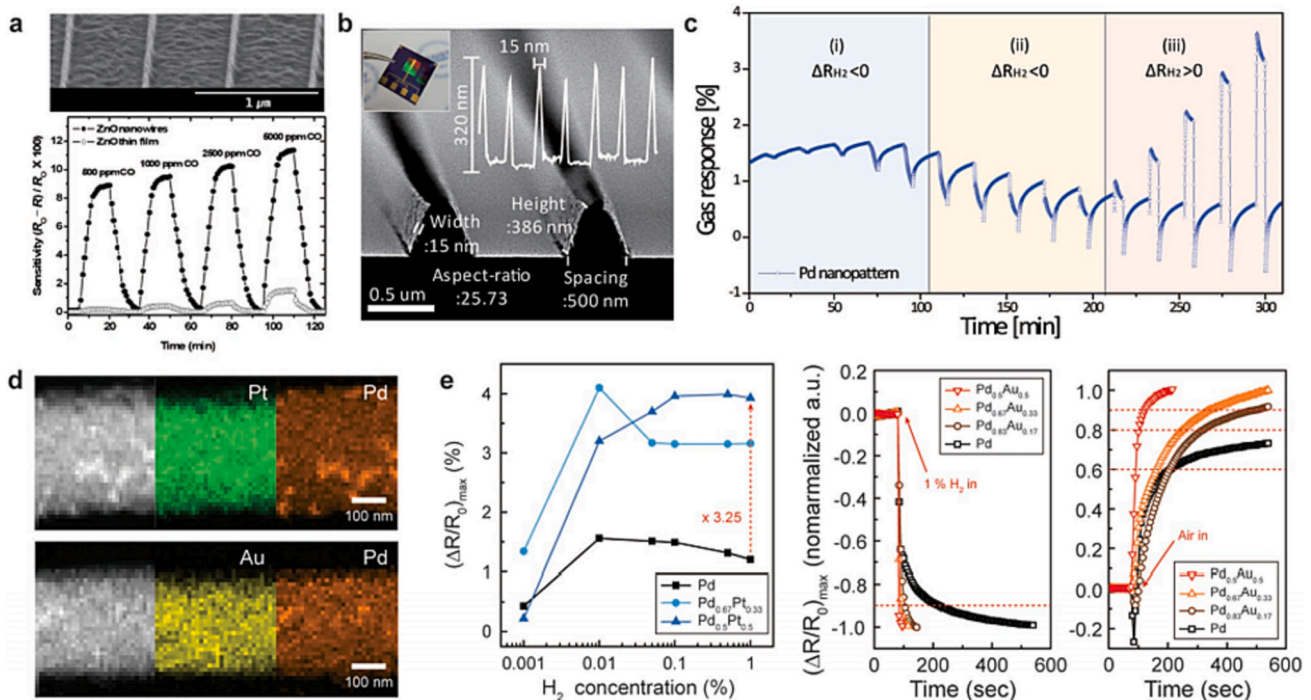


Fig. 12. High resolution and high aspect ratios gas sensors utilizing secondary and edge lithography. a) CO-based gas sensors of ZnO NW were designed and fabricated by spacer-lithography [143]. b) High resolution (16 nm) Pd nano-pattern for hydrogen gas sensors [174]. c) Dual switching sensor response of Pd nano-pattern rendering to hydrogen concentrations [174–176]. d) Well-blended Pd bi-metallic nano-pattern for improved hydrogen gas sensor [137]. e) Improved hydrogen sensor response in Pd–Pt bi-metallic hydrogen gas sensor and swift response times of the Pd–Au bi-metallic hydrogen gas sensors [178].

or surface catalysts. Tubular structures can be made to have different compositions in order to increase their sensitivity and selectivity to different gases and to provide a variety of specialized sensors depending on the target gases and application. In addition to these broad and qualitative justifications, it's important to remember that these characteristics also heavily depend on the material, how it was prepared, and the material itself—gaseous compounds should be assessed on a case-by-case basis.

Different MOX catalytic and electrochemical sensors fall into the detection range of 1 ppm to 1% limit (Fig. 13). Previous research has shown that a detection range of 100 ppb of HCHO and 20 ppb of naphthalene is successively achieved [180]. To increase the sensitivity and selectivity, further researchers have proposed a MOX sensor design with a porous sensing layer. The use of a porous sensing layer offers numerous active sites. These porous layers can be synthesized by chemical template-based methods [183]. The pore size and the film thickness can be tuned for developing potential MOX gas sensors with various compositions that affect sensing performance [184].

Polymer-based sensors are developed for monitoring healthcare and environmental pollutants [185]. Various capped nanoparticle sensors for volatile compounds detection have been investigated as chemiresistor sensors. Chemiresistor sensors have been designed with decorated Au nano-particle thin film platforms. Such chemiresistive sensors are used to detect volatile compounds and breath of lung cancer or diabetic patients under normal conditions. The advanced NEMS technology has made a possibility to design gas sensor platforms with different nanoparticles, compositions, and sizes to achieve better sensitivity and selectivity. In nanostructured sensors, the high sensitivity and selective response in gaseous mixtures of volatile compounds can be achieved with a LOD of 20 ppb [186].

Other conducting polymer sensors have also been widely employed for NEMS platforms. Doped conducting polypyrrole (PPy) with sulfonated groups have been designed for detecting explosive gases such as 2,4,6-trinitrotoluene (TNT). The sensing layer of PPy on Au-electrodes was electropolymerized in the presence of the sulfonated dyes as shown in Fig. 14. The sensor demonstrates high sensitivity and selectivity to TNT with a LOD of 0.2 ppb and 10–800 ppb, respectively [187].

CNTs are widely used for detecting NH_3 , NO_2 , and various organic compounds. A LOD of 44 and 262 ppb have been obtained for NO_2 and TNT, respectively [188]. MOSFET sensors have utilized CNTs to detect and improve selectivity among NO_2 , CO, CO_2 , O_2 , and H_2 [189,190]. Few researchers have shown that CNT sensors are not that efficient for the detection of CO, H_2O , and bimolecular due to their high bonding energy and ability to charge transfer to CNTs. Doping has been suggested to alleviate this problem, such as N_2 and B-doped CNTs are useful for room temperature selective detection of C_2H_2 , H_2O , and NO in a low concentration. B-doped CNTs are highly sensitive towards C_2H_2 , while N_2 -doped CNTs are more sensitive to NO_2 and CO [191].

Capacitive micromachined ultrasonic transducers sensors employing different layers of polyimide, amine- and quinidine have been used for CO_2 detection. The sensitivity of CO_2 detection around 1.06 ppm/Hz at 50 MHz has been obtained in the past. The sensitivity of CO_2 detectors can be affected by the presence of water vapor,

repeatability, and integration [192]. Other toxic gas sensors based on a cholesteric liquid crystal coated with fibers have been reported for the detection of tetrahydrofuran, acetone, and methanol gas, respectively. The sensitivity of such a sensor increases with the molar mass of the volatile compounds [193]. ZnO nano-particle has been used with the fiber-optic gas sensor for the detection of $\text{C}_3\text{H}_6\text{O}$, NH_3 , and $\text{C}_2\text{H}_5\text{OH}$. The ZnO nano-particles improve the sensitivity of NH_3 up to 150 ppm and $\text{C}_3\text{H}_6\text{O}$ at >150 ppm [194]. Such sensors are highly selective towards CO among a mixture of NH_3 , CO_2 , NO_x , LPG, and H_2 [195].

7. Relation between NEMS and gas sensors

Nanoelectromechanical systems, or NEMS for short, are promising prospects for a wide range of applications in fundamental science and semiconductor-based technologies [196,197]. Cells, proteins, and gas molecules are all weighed using precision mass sensors called NEMS resonators [198–200]. The NEMS mass sensor is based on observing the shift in the NEMS resonator's resonant frequency upon the absorption of an extra mass onto its surface. Due to the material's superior rigidity and low specific mass, graphene sheets are currently attracting a lot of interest for use as the foundation of NEMS resonators.

Previous study [201], presented a technique for producing high-quality free-standing graphene NEMS on a wide scale, wherein the supporting polymer constantly coats the graphene top surface during the construction process. Graphene is a highly sensitive material that is employed in research for gas sensing applications [201], but it can be even more sensitive with an efficient, one-step process.

NEMS that use mass transducing mechanisms function according to the frequency shift theory. Essentially, this means that resonance frequencies are found for both the system with and without connected nanoparticles. It is possible to roughly identify the type of chemical substance based on the difference between these two frequencies. Thus far, NEMS resonators built on graphene sheets have been utilized to study detection using basic chemical substances such H_2 , H_2O , O_2 , CO_2 , CO, NO_2 , Fe, Co, Ni, Ru, Rh, Pd, Os, Ir, and Pt from both a theoretical and experimental perspective [202]. While proof-of-principle comparative studies revealed that graphene, as a building block of a gas sensor, has a high sensitivity to gas molecules, graphene's detecting capabilities could be improved by employing a nanoporous substrate.

8. Conclusions, challenges, and future perspectives

In this comprehensive review, we have highlighted the recent advances and developments in the field of MEMS technology over the decades including various MEMS-based platforms and their fabrication techniques and materials, and various strategies to improve device performance.

1. Several advancements in this MEMS fabrication procedure from lithography to micromachining and new materials, internet of things (IoTs), and advanced BioMEMS are expected to revolutionize this area. Among gas sensors, MEMS has made impressive progress such as FET-based gas sensors and emerging, commercial applications are

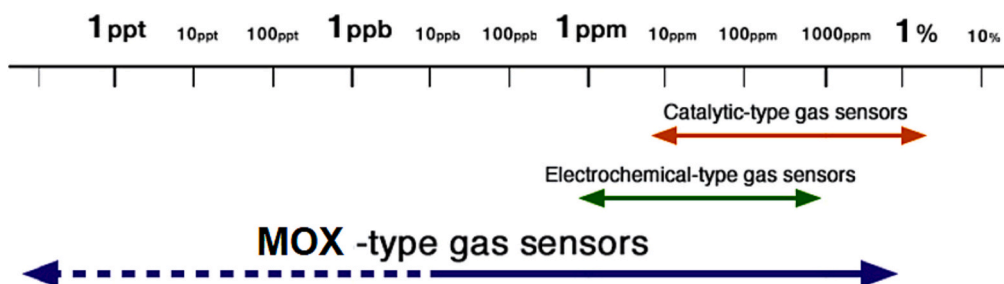


Fig. 13. Detection range of important MOX-based gas sensors [182].

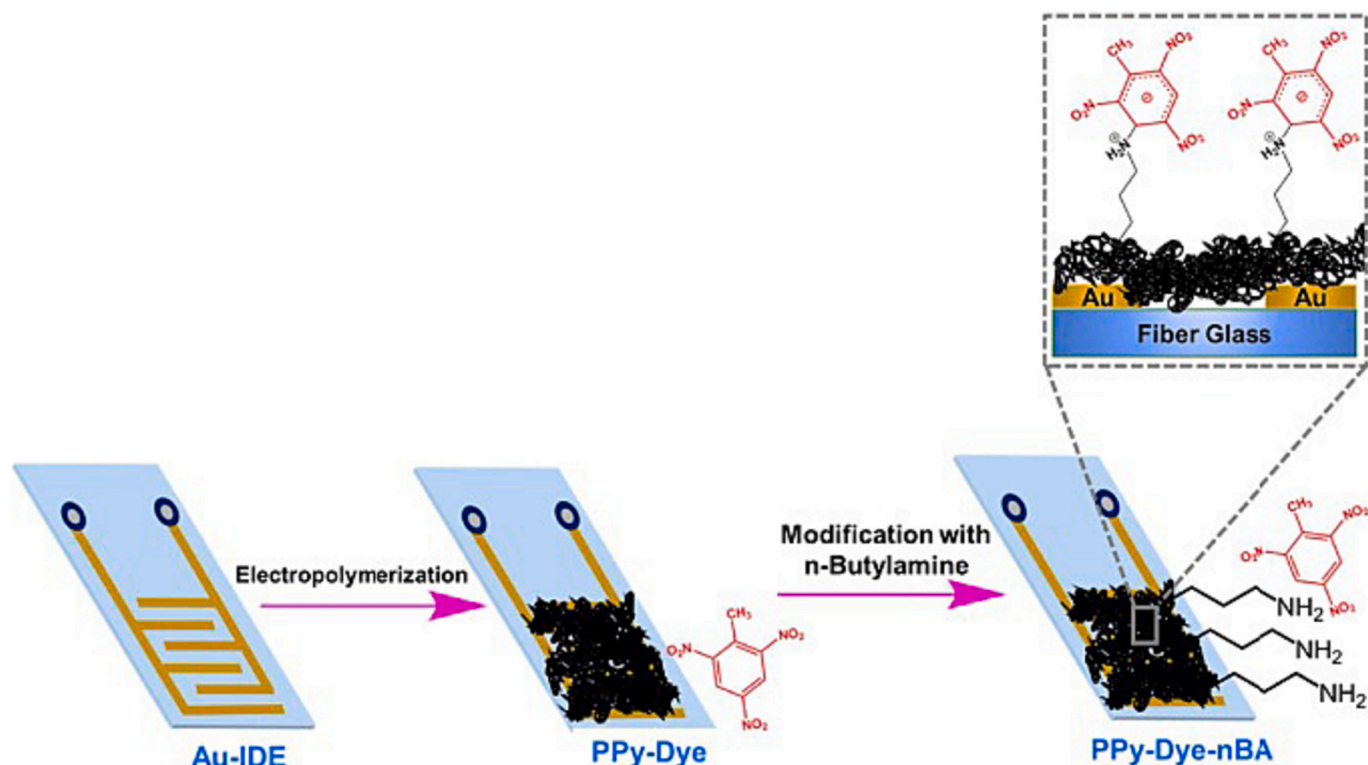


Fig. 14. Sensing mechanism of polymer gas sensor [187].

expected to benefit the materials community research for a wide usage of gas sensing technology.

- MEMS-based platforms have a simple organization, ease of fabrication, and are available in plenty. Emerging NEMS technology has not only reduced the final dimensions of the sensing device but also consumes less power. Future guidelines for improving the fabrication techniques, novel materials, and techniques, high-performance microdevices that can operate at room temperatures will be more readily available.
- The combination of the NEMS technique with the current MEMS will play an important role in laying the foundation of microdevice and gas sensors for smaller and low-cost sensors with improved performance and multi-functionality.
- The evolution of MEMS to NEMS during the last decades has a great potential to build a foundation for the upcoming technological revolution in miniaturized and flexible electronics.
- In the future, it is expected that these NEMS-based gas sensor technologies may replace MEMS owing to their superior performance, smaller dimension, and multi-functionalities.

Declaration of competing interest

The authors declare that they have no known competing financial interests or personal relationships that could have appeared to influence the work reported in this paper.

Data availability

The raw/processed data required to reproduce these findings cannot be shared at this time due to legal or ethical reasons.

References

- B. Sharma, A. Sharma, J.S. Kim, Recent advances on H₂ sensor technologies based on MOX and FET devices: a review, *Sensors Actuators B Chem.* 262 (2018) 758–770.
- J.W. Judy, *Microelectromechanical systems (MEMS): fabrication, design and applications*, *Smart Mater. Struct.* 10 (6) (2001) 1115.
- Y. Fu, H. Du, W. Huang, S. Zhang, M. Hu, TiNi-based thin films in MEMS applications: a review, *Sens. Actuators, A* 112 (2–3) (2004) 395–408.
- K. Tao, L. Tang, J. Wu, S.W. Lye, H. Chang, J. Miao, Investigation of multimodal electret-based MEMS energy harvester with impact-induced nonlinearity, *J. Microelectromech. Syst.* 27 (2) (2018) 276–288.
- J.L. Arlett, E.B. Myers, M.L. Roukes, Comparative advantages of mechanical biosensors, *Nat. Nanotechnol.* 6 (4) (2011) 20315.
- J.H. Kepper IV, B.C. Claus, J.C. Kinsey, A navigation solution using a MEMS IMU, model-based dead-reckoning, and one-way-travel-time acoustic range measurements for autonomous underwater vehicles, *IEEE J. Ocean. Eng.* 44 (3) (2018) 664–682.
- Y. Huang, E.L. Mather, J.L. Bell, M. Madou, MEMS-based sample preparation for molecular diagnostics, *Anal. Bioanal. Chem.* 372 (1) (2002) 49–65.
- M. Marzencki, Y. Ammar, S. Basrour, Integrated power harvesting system including a MEMS generator and a power management circuit, *Sens. Actuators, A* 145 (2008) 363–370.
- H.A. Yang, M. Wu, W. Fang, Localized induction heating solder bonding for wafer level MEMS packaging, *J. Microelectromech. Syst.* 15 (2) (2004) 394.
- J. Arab, D.K. Mishra, H.K. Kannoja, P. Adhale, P. Dixit, Fabrication of multiple through-holes in non-conductive materials by electrochemical discharge machining for RF MEMS packaging, *J. Mater. Process. Technol.* 271 (2019) 542–553.
- P. Bhattacharyya, P.K. Basu, B. Mondal, H. Saha, A low power MEMS gas sensor based on nanocrystalline ZnO thin films for sensing methane, *Microelectron. Reliab.* 48 (11–12) (2008) 1772–1779.
- T.J. Hsueh, C.H. Peng, W.S. Chen, A transparent ZnO nanowire MEMS gas sensor prepared by an ITO micro-heater, *Sensors Actuators B Chem.* 304 (2020) 127319.
- A. Bagolini, A. Gaiardo, M. Crivellari, E. Demenev, R. Bartali, A. Picciotto, M. Valt, F. Ficorella, V. Guidi, P. Bellutti, Development of MEMS MOS gas sensors with CMOS compatible PECVD inter-metal passivation, *Sensors Actuators B Chem.* 292 (2019) 225–232.
- H. Liu, L. Zhang, K.H.H. Li, O.K. Tan, Microhotplates for metal oxide semiconductor gas sensor applications—towards the CMOS-MEMS monolithic approach, *Micromachines* 9 (11) (2018) 557.
- G.S. Korotchenkov, *Handbook of gas Sensor materials properties, advantages and shortcomings for applications volume 1: Conventional approaches*, in: *Integrated Analytical Systems*, Springer, New York, NY, USA, 2013.
- P. Bhattacharyya, Technological journey towards reliable microheater development for MEMS gas sensors: a review, *IEEE Trans. Device Mater. Reliab.* 14 (2) (2014) 589–599.
- R.G. Spruijt, J.T. van Ommen, M.K. Ghatkesar, H.H.P. Garza, A review on development and optimization of microheaters for high-Temperature In Situ Studies, *J. Microelectromech. Syst.* 26 (6) (2017) 1165–1182.

- [18] I. Cho, K. Kang, D. Yang, J. Yun, I. Park, Localized liquid-phase synthesis of porous SnO₂ nanotubes on MEMS platform for low-power, high performance gas sensors, *ACS Appl. Mater. Interfaces* 9 (32) (2017) 27111–27119.
- [19] J. Zhu, M. Cho, Y. Li, I. Cho, J.H. Suh, D.D. Orbe, Y. Jeong, T.L. Ren, I. Park, Biomimetic turbinate-like artificial nose for hydrogen detection based on 3D porous laser-induced graphene, *ACS Appl. Mater. Interfaces* 11 (27) (2019) 24386–24394.
- [20] B. Sharma, J.S. Kim, MEMS based highly sensitive dual FET gas sensor using graphene decorated Pd-ag alloy nanoparticles for H₂ detection, *Sci. Rep.* 8 (1) (2018) 1–9.
- [21] T.J. Hsueh, C.H. Peng, W.S. Chen, A transparent ZnO nanowire MEMS gas sensor prepared by an ITO micro-heater, *Sensors Actuators B Chem.* 304 (2020) 127319.
- [22] V.V. Kondalkar, L.T. Duy, H. Seo, K. Lee, Nanohybrids of Pt-Functionalized Al₂O₃/ZnO Core-Shell Nanorods for High-Performance MEMS-Based Acetylene Gas Sensor, *ACS Appl. Mater. Interfaces* 11 (29) (2019) 25891–25900.
- [23] M. Gao, M. Cho, H.J. Han, Y.S. Jung, I. Park, Palladium-decorated silicon nanomesh fabricated by nanosphere lithography for high performance, room temperature hydrogen sensing, *Small* 14 (10) (2018) 1703691.
- [24] M. Cho, J. Yun, D. Kwon, K. Kim, I. Park, High-sensitivity and low-power flexible schottky hydrogen sensor based on silicon nanomembrane, *ACS Appl. Mater. Interfaces* 10 (15) (2018) 12870–12877.
- [25] D. Hasan, C. Lee, Hybrid metamaterial absorber platform for sensing of CO₂ gas at mid-IR, *Adv. Sci.* 5 (5) (2018) 1700581.
- [26] D. Matatagui, A. Sainz-Vidal, I. Gràcia, E. Figueras, C. Cané, J.M. Saniger, Chemosensitive gas sensor based on ZIF-8/ZIF-67 nanocrystals, *Sensors Actuators B Chem.* 274 (2018) 601–608.
- [27] T.J. Hsueh, C.L. Lu, A hybrid YSZ/SnO₂/MEMS SO₂ gas sensor, *RSC Adv.* 9 (48) (2019) 27800–27806.
- [28] D. Im, D. Kim, D. Jeong, W.I. Park, M. Chun, J.S. Park, H. Kim, H. Jung, Improved formaldehyde gas sensing properties of well-controlled au nanoparticle-decorated In₂O₃ nanofibers integrated on low power MEMS platform, *J. Mater. Sci. Technol.* 38 (2020) 56–63.
- [29] Y. Wang, C. Liu, Z. Wang, Z. Song, X. Zhou, N. Han, Y. Chen, Sputtered SnO₂: NiO thin films on self-assembled au nanoparticle arrays for MEMS compatible NO₂ gas sensors, *Sensors Actuators B Chem.* 278 (2019) 28–38.
- [30] B. Behera, S. Chandra, An innovative gas sensor incorporating ZnO–CuO nanoflakes in planar MEMS technology, *Sensors Actuators B Chem.* 229 (2016) 414–424.
- [31] W. Yan, H. Xu, M. Ling, S. Zhou, T. Qiu, Y. Deng, Z. Zhao, E. Zhang, MOF-Derived Porous Hollow Co₃O₄@ZnO Cages for High-Performance MEMS Trimethylamine Sensors vol. 6, *ACS Sens.* 2021, pp. 2613–2621.
- [32] M. Li, W. Luo, X. Liu, G. Niu, F. Wang, Wafer-Level Patterning of SnO Nanosheets for MEMS Gas Sensors, *IEEE Electron Dev. Lett.* 43 (11) (1981–1984).
- [33] K. Suematsu, W. Harano, T. Oyama, N. Ma, K. Watanabe, K. Shimano, Ultra-High Sensitive Gas Detection Using Pulse-Driven Mems Sensor Based on Tin Dioxide 2019, *IEEE international symposium on olfaction and electronic nose (ISOEN)*, Fukuoka, Japan, 2019, pp. 1–3.
- [34] T.A. Kunt, T.J. McAvoy, R.E. Cavicchi, S. Semancik, Optimization of temperature programmed sensing for gas identification using micro-hotplate sensors, *Sensor Actuat B-Chem* 53 (1–2) (1998) 24–43.
- [35] J. Lee, C.M. Spadaccini, E.V. Mukerjee, W.P. King, Differential scanning calorimeter based on suspended membrane single crystal silicon microhotplate, *J. Microelectromech. S.* 17 (6) (2008) 1513–1525.
- [36] L. Xu, T. Li, X.L. Gao, Y.L. Wang, Development of a reliable micro-hotplate with low power consumption, *IEEE Sensors J.* 11 (4) (2011) 913–919.
- [37] I. Elmi, S. Zampolli, E. Cozzani, F. Mancarella, G.C. Cardinali, Development of ultra-low-power consumption MOX sensors with ppb-level VOC detection capabilities for emerging applications, *Sensor Actuat B-Chem* 135 (1) (2008) 342–351.
- [38] L. Xu, T. Li, Y.L. Wang, A novel three-dimensional microheater, *IEEE Electr Device L* 32 (9) (2011) 1284–1286.
- [39] K. Suematsu, Y. Hiroshima, W. Harano, W. Mizukami, K. Watanabe, K. Shimano, Double-step modulation of the Pulse-Driven mode for a high-performance SnO₂ Micro gas Sensor: designing the particle surface via a rapid preheating process, *ACS Sens.* 5 (11) (2020) 3449–3456.
- [40] A.A. Vasiliev, A.V. Pislakov, A.V. Sokolov, N.N. Samotae, S.A. Soloviev, K. Oblov, V. Guarnieri, L. Lorenzelli, J. Brunelli, A. Maglione, A.S. Lipilin, Non-silicon MEMS platforms for gas sensors, *Sensors Actuators B Chem.* 224 (2016) 700–713.
- [41] Tzu-Sen Yang, Jin-Chern Chiou, A high-efficiency driver circuit for a gas-Sensor microheater Based on a switch-mode DC-to-DC converter, *Sensors* 20 (2020) 5367.
- [42] M.I.A. Asri, M.N. Hasan, M.R.A. Fuaad, M.S.M. Ali, MEMS gas sensors: a review, *IEEE Sensors J.* 21 (17) (2021) 18281–18397.
- [43] M.T. Sebastian, H. Jantunen, Low loss dielectric materials for LTCC applications: a review, *Int. Mater. Rev.* 53 (2) (2008) 57–90.
- [44] J. Ortigoza-Diaz, K. Scholten, C. Larson, A. Cobo, T. Hudson, J. Yoo, A. Baldwin, A. Weltman Hirschberg, E. Meng, Techniques and considerations in the microfabrication of Parylene C microelectromechanical systems, *Micromachines* 9 (9) (2018) 422.
- [45] D. Thuau, P.H. Ducrot, P. Poulin, I. Dufour, C. Ayela, Integrated electromechanical transduction schemes for polymer MEMS sensors, *Micromachines* 9 (5) (2018) 197.
- [46] T.R. Rashid, D.T. Phan, G.S. Chung, Effect of Ga-modified layer on flexible hydrogen sensor using ZnO nanorods decorated by Pd catalysts, *Sensors Actuators B Chem.* 193 (2014) 869–876.
- [47] T.M. Perfecto, C.A. Zito, T. Mazon, D.P. Volanti, Flexible room-temperature volatile organic compound sensors based on reduced graphene oxide–WO₃·0.33H₂O nano-needles, *J. Mater. Chem. C* 6 (11) (2018) 2822–2829.
- [48] A.I. Uddin, G.S. Chung, Effects of ag nanoparticles decorated on ZnO nanorods under visible light illumination on flexible acetylene gas sensing properties, *J. Electroceram.* 40 (1) (2018) 42–49.
- [49] S.M. Mohammad, Z. Hassan, R.A. Talib, N.M. Ahmed, M.A. Al-Azawi, N.M. Abd-Alghafour, C.W. Chin, N.H. Al-Hardan, Fabrication of a highly flexible low-cost H₂ gas sensor using ZnO nanorods grown on an ultra-thin nylon substrate, *J. Mater. Sci. Mater. Electron.* 27 (9) (2016) 9461–9469.
- [50] M. Seetha, P. Meena, D. Mangalaraj, Y. Masuda, K. Senthil, Synthesis of indium oxide cubic crystals by modified hydrothermal route for application in room temperature flexible ethanol sensors, *Mater. Chem. Phys.* 133 (1) (2012) 47–54.
- [51] B. Degroote, R. Rooyackers, T. Vandeweyer, N. Collaert, W. Boullart, E. Kunnen, D. Shamiryan, J. Wouters, J. Van Puymbroek, A. Dixit, M. Jurczak, Spacer defined FinFET: active area patterning of sub-20 nm fins with high density, *Microelectron. Eng.* 84 (4) (2007) 609–618.
- [52] J. Hållstedt, P.E. Hellström, H.H. Radamson, Sidewall transfer lithography for reliable fabrication of nanowires and deca-nanometer MOSFETs, *Thin Solid Films* 517 (1) (2008) 117–120.
- [53] Y. Mo, Y. Okawa, M. Tajima, T. Nakai, N. Yoshiike, K. Natukawa, Micro-machined gas sensor array based on metal film micro-heater, *Sensors Actuators B Chem.* 79 (2–3) (2001) 175–181.
- [54] J.L. Fu, F. Ayazi, High-Q Q \$ \$ AlN-on-silicon resonators with annexed platforms for portable integrated VOC sensing, *J. Microelectromech. Syst.* 24 (2) (2014) 503–509.
- [55] R.K. Rose, C.W. Woodson, Mechanical Technology Inc, Application of organic gas sensors in the detection and separation of recovered volatile organic compounds (VOCs), *U.S. Patent* 5 (1995) 435,141.
- [56] R. Bogue, Nanosensors: a review of recent research, *Sens. Rev.* 29 (4) (2009) 310–315.
- [57] J. Guo, J. Zhang, M. Zhu, D. Ju, H. Xu, B. Cao, High-performance gas sensor based on ZnO nanowires functionalized by au nanoparticles, *Sensors Actuators B Chem.* 199 (2014) 339–345.
- [58] Q. Zhou, A. Sussman, J. Chang, J. Dong, A. Zettl, W. Mickelson, Fast response integrated MEMS microheaters for ultra low power gas detection, *Sens. Actuators, A* 223 (2015) 67–75.
- [59] P. Karnati, J. Walker, M. Al-Hashem, D. Miller, S. Akbar, P. Morris, Comparison of electrical measurements of nanostructured gas sensors using wire bonding vs. probe station. *Meas.* 153 (2020) 107451.
- [60] R. Bogue, Recent developments in MEMS sensors: a review of applications, markets and technologies, *Sens. Rev.* 33 (4) (2013) 300–304.
- [61] M. Liao, Y. Koide, Carbon-based materials: growth, properties, MEMS/NEMS technologies, and MEM/NEM switches, *Crit. Rev. Solid State Mater. Sci.* 36 (2) (2011) 66–101.
- [62] K. Eom, H.S. Park, D.S. Yoon, et al., Nanomechanical resonators and their applications in biological/chemical detection: nanomechanics principles, *Phys. Rep.* 503 (2011) 115–163.
- [63] J.L. Arlett, J.R. Maloney, B. Gudlewski, et al., Self-sensing micro and nanocantilevers with Attonewton-scale force resolution, *Nano Lett.* 6 (2006) 1000–1006.
- [64] D. Rugar, R. Budakian, H.J. Mamin, et al., Single spin detection by magnetic resonance force microscopy, *Nature* 430 (2004) 329–332.
- [65] K.L. Ekinci, X.M.H. Huang, M.L. Roukes, Ultrasonically nanoelectromechanical mass detection, *Appl. Phys. Lett.* 84 (2004) 4469–4471.
- [66] Y.T. Yang, C. Callegari, X.L. Feng, et al., Zeptogram-scale nanomechanical mass sensing, *Nano Lett.* 6 (2006) 583–586.
- [67] J. Chaste, et al., A nanomechanical mass sensor with yoctogram resolution, *Nat. Nanotechnol.* 7 (2012) 301–304.
- [68] L. Duraffourg, J. Arcamone, From MEMS to NEMS, in: *Nanoelectromechanical Systems*, John Wiley and Sons, 2015.
- [69] S. Fanget, S. Hentz, P. Puget, J. Arcamone, M. Matheron, E.D. Colinet, P. Andreucci, L. Duraffourg, E. Myers, M.L. Roukes, Gas sensors based on gravimetric detection—a review, *Sensors Actuators B Chem.* 160 (1) (2011) 804–821.
- [70] I. Bargatini, E.B. Myers, J.S. Aldridge, C. Marcoux, P. Brianseau, L. Duraffourg, E. Colinet, S. Hentz, P. Andreucci, M.L. Roukes, Large-scale integration of nanoelectromechanical systems for gas sensing applications, *Nano Lett.* 12 (3) (2012) 1269–1274.
- [71] S.M. Allameh, W.O. Soboyejo, T.S. Srivatsan, Silicon-based microelectromechanical systems (si-MEMS), *Mater. Engineer.-New York* 32 (2006) 65.
- [72] Y.P. Wong, S. Lorenzo, Y. Miao, J. Bregman, O. Solgaard, Extended design space of silicon-on-nothing MEMS, *J. Microelectromech. Syst.* 28 (5) (2019) 850–858.
- [73] S. Herberger, M. Herold, H. Ulmer, A. Burdack-Freitag, F. Mayer, Detection of human effluents by a MOS gas sensor in correlation to VOC quantification by GC/MS, *Build. Environ.* 45 (11) (2010) 2430–2439.
- [74] A.A. Vasiliev, A.V. Pislakov, M. Zen, B. Margesin, V. Guarnieri, F. Giacomozzi, S. Brida, G. Soncini, D. Vincenzi, G. Martinelli, M.C. Carotta, Membrane-type gas sensor with thick film sensing layer: optimization of heat losses, in: *Eurosensors XIV, The 14th European Conference on Solid-State Transducers*, 2000, pp. 213–214. MIC-Mikroelektronik Centre.
- [75] D. Vincenzi, M.A. Butturi, V. Guidi, M.C. Carotta, G. Martinelli, V. Guarnieri, S. Brida, B. Margesin, F. Giacomozzi, M. Zen, G.U. Pignatelli, Development of a low-power thick-film gas sensor deposited by screen-printing technique onto a micromachined hotplate, *Sensors Actuators B Chem.* 77 (1–2) (2001) 95–99.

- [76] A. Vila, J. Puigcorbe, D. Vogel, B. Michel, N. Sabate, I. Gracia, C. Cane, J. R. Morante, Reliability analysis of Pt-Ti micro-hotplates operated at high temperature, in: Euroensors XVII, University of Guimaraes, Guimaraes, Portugal, 2003 p.250–p.253.
- [77] A. Vasiliev, R. Pavelko, S. Gogish-Klushin, D. Kharitonov, O. Gogish-Klushina, A. Pislakov, A. Sokolov, N. Samotaev, V. Guarnieri, M. Zen, L. Lorenzelli, Sensors based on technology “nano-on-micro” for wireless instruments preventing ecological and industrial catastrophes, in: M.-I. Baraton (Ed.), Sensors for Environment, The Netherlands, Health and Security, Springer, Dordrecht, 2009, pp. 205–228.
- [78] A.A. Vasiliev, A.M. Baranov, A.V. Sokolov, Method of the deposition of platinum layers onto substrate, in: Patent of Russian Federation # 2426193, 2010 priority 05.05.
- [79] V.A. Iovdalsky, I.M. Olikhov, I.M. Bleivas, V.M. Ipolitov, Samsung Electronics Co Ltd, Hybrid Integrated Circuit For a Gas Sensor, 2001. U.S. Patent 6,202,467.
- [80] Tetrycz, H., Kita, J., Bauer, R., Golonka, L., Licznarski, B.W., Nitsch, K. and Wisniewski, K., 1998. New design of an SnO₂ gas sensor on low temperature cofiring ceramics. *Sensors Actuators B Chem.*, 47(1–3), pp.100–103.
- [81] J. Kita, A. Dzedzic, L.J. Golonka, A. Bochenek, Properties of laser cut LTCC heaters, *Microelectron. Reliab.* 40 (6) (2000) 1005–1010.
- [82] A.A. Vasiliev, A.V. Pislakov, A.V. Sokolov, N.N. Samotaev, S.A. Soloviev, K. Oblov, V. Guarnieri, L. Lorenzelli, J. Brunelli, A. Maglione, A.S. Lipilin, Non-silicon MEMS platforms for gas sensors, *Sensors Actuators B Chem.* 224 (2016) 700–713.
- [83] Tzu-Sen Yang, Jin-Chern Chiou, A high-efficiency driver circuit for a gas-Sensor microheater Based on a switch-mode DC-to-DC converter, *Sensors* 20 (2020) 5367.
- [84] S.M. Majhi, A. Mirzaei, H.W. Kim, S.S. Kim, T.W. Kim, Recent advances in energy-saving chemiresistive gas sensors: A review, *Nano Energy* 79 (2021) 105369.
- [85] M.I.A. Asri, M.N. Hasan, M.R.A. Fuaad, M.S.M. Ali, MEMS gas sensors: a review, *IEEE Sensors J.* 21 (17) (2021) 18281–18397.
- [86] A.A. Vasiliev, R.G. Pavelko, S.Y. Gogish-Klushin, D.Y. Kharitonov, O.S. Gogish-Klushina, A.V. Sokolov, A.V. Pislakov, N.N. Samotaev, Alumina MEMS platform for impulse semiconductor and IR optic gas sensors, *Sensors Actuators B Chem.* 132 (1) (2008) 216–223.
- [87] SGX Sensortech, Switzerland. <http://www.sgxsensortech.com>, 2024.
- [88] A. Mozalev, S. Magaino, H. Imai, The formation of nanoporous membranes from anodically oxidized aluminium and their application to Li rechargeable batteries, *Electrochim. Acta* 46 (18) (2001) 2825–2834.
- [89] X. Chen, Z. Guo, J. Huang, F. Meng, M. Zhang, J. Liu, Fabrication of gas ionization sensors using well-aligned MWCNT arrays grown in porous AAO templates. *Colloids surf. A* 313 (2008) 355–358.
- [90] F. Rumiche, H.H. Wang, W.S. Hu, J.E. Indacochea, M.L. Wang, Anodized aluminum oxide (AAO) nanowell sensors for hydrogen detection, *Sensors Actuators B Chem.* 134 (2) (2008) 869–877.
- [91] C. Li, M. Zheng, X. Wang, L. Yao, L. Ma, W. Shen, Fabrication and ultraviolet photoresponse characteristics of ordered SnO_x (x = 0.87, 1.45, 2) nanopore films, *Nanoscale Res. Lett.* 6 (1) (2011) 615.
- [92] N. Kumar, A.K. Srivastava, R. Nath, B.K. Gupta, G.D. Varma, Probing the highly efficient room temperature ammonia gas sensing properties of a luminescent ZnO nanowire array prepared via an AAO-assisted template route, *Dalton Trans.* 43 (15) (2014) 5713–5720.
- [93] N. Taşaltun, S. Öztürk, N. Kılınc, Z.Z. Öztürk, Investigation of the hydrogen gas sensing properties of nanoporous Pd alloy films based on AAO templates, *J. Alloys Compd.* 509 (14) (2011) 4701–4706.
- [94] E. Di Bartolomeo, M.L. Grilli, N. Antonias, S. Cordiner, E. Traversa, Testing planar gas sensors based on yttria-stabilized zirconia with oxide electrodes in the exhaust gases of a spark ignition engine, *Sens. Lett.* 3 (1–2) (2005) 22–26.
- [95] J.W. Fergus, Materials for high temperature electrochemical NO_x gas sensors, *Sensors Actuators B Chem.* 121 (2) (2007) 652–663.
- [96] S. Yu, Q. Wu, M. Tabib-Azar, C.C. Liu, Development of a silicon-based yttria-stabilized-zirconia (YSZ), amperometric oxygen sensor, *Sensors Actuators B Chem.* 85 (3) (2002) 212–218.
- [97] N.J. Dayan, S.R. Sainkar, R.N. Karekar, R.C. Aiyer, Formulation and characterization of ZnO: Sb thick-film gas sensors, *Thin Solid Films* 325 (1–2) (1998) 254–258.
- [98] A. Chowdhuri, V. Gupta, K. Sreenivas, R. Kumar, S. Mozumdar, P.K. Patanjali, Response speed of SnO₂-based H₂ S gas sensors with CuO nanoparticles, *Appl. Phys. Lett.* 84 (7) (2004) 1180–1182.
- [99] M.T. Sebastian, H. Jantunen, Low loss dielectric materials for LTCC applications: a review, *Int. Mater. Rev.* 53 (2) (2008) 57–90.
- [100] J. Ortigoza-Diaz, K. Scholten, C. Larson, A. Cobo, T. Hudson, J. Yoo, A. Baldwin, A. Weltman Hirschberg, E. Meng, Techniques and considerations in the microfabrication of Parylene C microelectromechanical systems, *Micromachines* 9 (9) (2018) 422.
- [101] D. Thuau, P.H. Ducrot, P. Poulin, I. Dufour, C. Ayela, Integrated electromechanical transduction schemes for polymer MEMS sensors, *Micromachines* 9 (5) (2018) 197.
- [102] I.H. Song, T. Park, PMMA solution assisted room temperature bonding for PMMA-PC hybrid devices, *Micromachines* 8 (9) (2017) 284.
- [103] Y. Seekaew, S. Lokavee, D. Phokharatkul, A. Wisitsoraat, T. Kerdraroen, C. Wongchoosuk, Low-cost and flexible printed graphene-PEDOT: PSS gas sensor for ammonia detection, *Org. Electron.* 15 (11) (2014) 2971–2981.
- [104] W.L. Ong, C. Zhang, G.W. Ho, Ammonia plasma modification towards a rapid and low temperature approach for tuning electrical conductivity of ZnO nanowires on flexible substrates, *Nanoscale* 3 (10) (2011) 4206–4214.
- [105] T.R. Rashid, D.T. Phan, G.S. Chung, Effect of Ga-modified layer on flexible hydrogen sensor using ZnO nanorods decorated by Pd catalysts, *Sensors Actuators B Chem.* 193 (2014) 869–876.
- [106] T.R. Rashid, D.T. Phan, G.S. Chung, A flexible hydrogen sensor based on Pd nanoparticles decorated ZnO nanorods grown on polyimide tape, *Sensors Actuators B Chem.* 185 (2013) 777–784.
- [107] R. Li, K. Jiang, S. Chen, Z. Lou, T. Huang, D. Chen, G. Shen, SnO₂/SnS₂ nanotubes for flexible room-temperature NH₃ gas sensors, *RSC Adv.* 7 (83) (2017) 52503–52509.
- [108] S. Li, P. Lin, L. Zhao, C. Wang, D. Liu, F. Liu, P. Sun, X. Liang, F. Liu, X. Yan, Y. Gao, The room temperature gas sensor based on polyaniline@flower-like WO₃ nanocomposites and flexible PET substrate for NH₃ detection, *Sensors Actuators B Chem.* 259 (2018) 505–513.
- [109] D.K. Subbiah, G.K. Mani, K.J. Babu, A. Das, J.B.B. Rayappan, Nanostructured ZnO on cotton fabrics—a novel flexible gas sensor & UV filter, *J. Clean. Prod.* 194 (2018) 372–382.
- [110] S. Li, Y. Diao, Z. Yang, J. He, J. Wang, C. Liu, F. Liu, H. Lu, X. Yan, P. Sun, G. Lu, Enhanced room temperature gas sensor based on au-loaded mesoporous In₂O₃ protected core-shell nanohybrid assembled on flexible PET substrate for NH₃ detection, *Sensors Actuators B Chem.* 276 (2018) 526–533.
- [111] H.Y. Li, C.S. Lee, D.H. Kim, J.H. Lee, Flexible room-temperature NH₃ sensor for ultrasensitive, selective, and humidity-independent gas detection, *ACS Appl. Mater. Interfaces* 10 (33) (2018) 27858–27867.
- [112] C. Liu, H. Tai, P. Zhang, Z. Yuan, X. Du, G. Xie, Y. Jiang, A high-performance flexible gas sensor based on self-assembled PANI-CeO₂ nanocomposite thin film for trace-level NH₃ detection at room temperature, *Sensors Actuators B Chem.* 261 (2018) 587–597.
- [113] X. Geng, C. Zhang, Y. Luo, M. Debliqy, Flexible NO₂ gas sensors based on sheet-like hierarchical ZnO_{1-x} coatings deposited on polypropylene papers by suspension flame spraying, *J. Taiwan Inst. Chem. Eng.* 75 (2017) 280–286.
- [114] U. Yaqoob, A.I. Uddin, G.S. Chung, A high-performance flexible NO₂ sensor based on WO₃ NPs decorated on MWCNTs and RGO hybrids on PI/PET substrates, *Sensors Actuators B Chem.* 224 (2016) 738–746.
- [115] C. Hua, Y. Shang, Y. Wang, J. Xu, Y. Zhang, X. Li, A. Cao, A flexible gas sensor based on single-walled carbon nanotube-Fe₂O₃ composite film, *Appl. Surf. Sci.* 405 (2017) 405–411.
- [116] T.M. Perfecto, C.A. Zito, T. Mazon, D.P. Volanti, Flexible room-temperature volatile organic compound sensors based on reduced graphene oxide-WO₃-0.33H₂O nano-needles, *J. Mater. Chem. C* 6 (11) (2018) 2822–2829.
- [117] A.I. Uddin, G.S. Chung, Effects of ag nanoparticles decorated on ZnO nanorods under visible light illumination on flexible acetylene gas sensing properties, *J. Electroceram.* 40 (1) (2018) 42–49.
- [118] S.M. Mohammad, Z. Hassan, R.A. Talib, N.M. Ahmed, M.A. Al-Azawi, N.M. Abd-Alghafour, C.W. Chin, N.H. Al-Hardan, Fabrication of a highly flexible low-cost H₂ gas sensor using ZnO nanorods grown on an ultra-thin nylon substrate, *J. Mater. Sci. Mater. Electron.* 27 (9) (2016) 9461–9469.
- [119] M. Seetha, P. Meena, D. Mangalaraj, Y. Masuda, K. Senthil, Synthesis of indium oxide cubic crystals by modified hydrothermal route for application in room temperature flexible ethanol sensors, *Mater. Chem. Phys.* 133 (1) (2012) 47–54.
- [120] C. Liu, Recent developments in polymer MEMS, *Adv. Mater.* 19 (22) (2007) 3783–3790.
- [121] H. Bai, G. Shi, Gas sensors based on conducting polymers, *Sens* 7 (3) (2007) 267–307.
- [122] W. Lamperska, S. Drobczyński, M. Nawrot, P. Wasylczyk, J. Masajada, Microdumbbells—a versatile tool for optical tweezers, *Micromachines* 9 (2018) 277.
- [123] Y. Seekaew, S. Lokavee, D. Phokharatkul, A. Wisitsoraat, T. Kerdraroen, C. Wongchoosuk, Low-cost and flexible printed graphene-PEDOT: PSS gas sensor for ammonia detection, *Org. Electron.* 15 (11) (2014) 2971–2981.
- [124] J. Jinsol, L. Jungchul, Design, fabrication, and characterization of liquid metal microheaters, *J. Microelectromech. Syst.* 23 (2014) 5.
- [125] T. Guan, R. Puers, Thermal analysis of a ag/Ti Based microheater, *Process. Eng.* 5 (2010) 1356–1359.
- [126] K.L. Zhang, S.K. Chou, S.S. Ang, Fabrication, modeling and testing of a thin film au/Ti microheater, *Int. J. Therm. Sci.* 46 (2007) 580–588.
- [127] R. Prajesh, V. Goyal, V. Saini, J. Bhargava, A. Sharma, A. Agarwal, *Microsyst. Technol.* 25 (2019) 9.
- [128] S.M. Park, M.P. Stoykovich, R. Ruiz, Y. Zhang, C.T. Black, P.F. Nealey, Directed assembly of lamellae-forming block copolymers by using chemically and topographically patterned substrates, *Adv. Mater.* 19 (4) (2007) 607–611.
- [129] D.E. Angelescu, J.H. Waller, D.H. Adamson, P. Deshpande, S.Y. Chou, R. A. Register, P.M. Chaikin, Macroscopic orientation of block copolymer cylinders in single-layer films by shearing, *Adv. Mater.* 16 (19) (2004) 1736–1740.
- [130] S.H. Park, D.O. Shin, B.H. Kim, D.K. Yoon, K. Kim, S.Y. Lee, S.H. Oh, S.W. Choi, S. C. Jeon, S.O. Kim, Block copolymer multiple patterning integrated with conventional ArF lithography, *Soft Matter* 6 (1) (2010) 120–125.
- [131] K. Kwon, J.M. Ok, Y.H. Kim, J.S. Kim, W.B. Jung, S.Y. Cho, H.T. Jung, Direct observation of highly ordered dendrimer soft building blocks over a large area, *Nano Lett.* 15 (11) (2015) 7552–7557.
- [132] T. Wang, J. Zhang, X. Zhang, P. Xue, H. Chen, X. Li, Y. Yu, B. Yang, Morphology-controlled fabrication of elliptical nanoring arrays based on facile colloidal lithography, *J. Mater. Chem. C* 1 (6) (2013) 1122–1129.
- [133] T. Wang, Z. Jiao, T. Chen, Y. Li, W. Ren, S. Lin, G. Lu, J. Ye, Y. Bi, Vertically aligned ZnO nanowire arrays tip-grafted with silver nanoparticles for photoelectrochemical applications, *Nanoscale* 5 (16) (2013) 7552–7557.

- [134] M.D. Levenson, N.S. Viswanathan, R.A. Simpson, Improving resolution in photolithography with a phase-shifting mask, *IEEE Trans. Electron Dev.* 29 (12) (1982) 1828–1836.
- [135] Y.K. Choi, T.J. King, C. Hu, A spacer patterning technology for nanoscale CMOS, *IEEE Trans. Electron Dev.* 49 (3) (2002) 436–441.
- [136] J. Hällstedt, P.E. Hellström, Z. Zhang, B.G. Malm, J. Edholm, J. Lu, S.L. Zhang, H. H. Radamson, M. Östling, A robust spacer gate process for deca-nanometer high-frequency MOSFETs, *Microelectron. Eng.* 83 (3) (2006) 434–439.
- [137] W.B. Jung, S. Jang, S.Y. Cho, H.J. Jeon, H.T. Jung, Recent progress in simple and cost-effective top-down lithography for ≈ 10 nm scale nanopatterns: from edge lithography to secondary sputtering lithography, *Adv. Mater.* 1907101 (2020).
- [138] L.E. Dodd, M.C. Rosamond, A.J. Gallant, D. Wood, Development of phase shift lithography for the production of metal-oxide-metal diodes, *Micro Nano Lett.* 9 (7) (2014) 437–440.
- [139] K. Subannajui, F. Güder, M. Zacharias, Bringing order to the world of nanowire devices by phase shift lithography, *Nano Lett.* 11 (9) (2011) 3513–3518.
- [140] F. Güder, Y. Yang, M. Kruger, G.B. Stevens, M. Zacharias, Atomic layer deposition on phase-shift lithography generated photoresist patterns for 1D nanochannel fabrication, *ACS Appl. Mater. Interfaces* 2 (12) (2010) 3473–3478.
- [141] J. Hu, T. Deng, R.G. Beck, R.M. Westervelt, K.D. Maranowski, A.C. Gossard, G. M. Whitesides, Fabrication of GaAs/AlGaAs high electron mobility transistors with 250 nm gates using conformal phase shift lithography, *Sens. Actuators, A* 86 (1–2) (2000) 122–126.
- [142] S.H. Chan, A.K. Wong, E.Y. Lam, Initialization for robust inverse synthesis of phase-shifting masks in optical projection lithography, *Opt. Express* 16 (19) (2008) 14746–14760.
- [143] J. Wu, C. Liow, K. Tao, Y. Guo, X. Wang, J. Miao, Large-area sub-wavelength optical patterning via long-range ordered polymer lens array, *ACS Appl. Mater. Interfaces* 8 (25) (2016) 16368–16378.
- [144] K. Subannajui, F. Güder, J. Danhof, A. Menzel, Y. Yang, L. Kirste, C. Wang, V. Cimalla, U. Schwarz, M. Zacharias, An advanced fabrication method of highly ordered ZnO nanowire arrays on silicon substrates by atomic layer deposition, *Nanotechnol* 23 (23) (2012) 235607.
- [145] K. Subannajui, F. Güder, M. Zacharias, Bringing order to the world of nanowire devices by phase shift lithography, *Nano Lett.* 11 (9) (2011) 3513–3518.
- [146] B. Degroote, R. Rooyackers, T. Vandeweyer, N. Collaert, W. Boullart, E. Kunnen, D. Shamiryan, J. Wouters, J. Van Puymbroeck, A. Dixit, M. Jurczak, Spacer defined FinFET: active area patterning of sub-20 nm fins with high density, *Microelectron. Eng.* 84 (4) (2007) 609–618.
- [147] J. Hällstedt, P.E. Hellström, H.H. Radamson, Sidewall transfer lithography for reliable fabrication of nanowires and deca-nanometer MOSFETs, *Thin Solid Films* 517 (1) (2008) 117–120.
- [148] C.Y. Hsiao, C.H. Lin, C.H. Hung, C.J. Su, Y.R. Lo, C.C. Lee, H.C. Lin, F.H. Ko, T. Y. Huang, Y.S. Yang, Novel poly-silicon nanowire field effect transistor for biosensing application, *Biosens. Bioelectron.* 24 (5) (2009) 1223–1229.
- [149] T. Huynh-Bao, J. Ryckaert, Z. Tókei, A. Mercha, D. Verkest, A.V.Y. Thean, P. Wambacq, Statistical timing analysis considering device and interconnect variability for BEOL requirements in the 5-nm node and beyond, *IEEE Trans. Very Large Scale Integr. VLSI Syst.* 25 (5) (2017) 1669–1680.
- [150] H. Noma, H. Kawata, M. Yasuda, Y. Hirai, J. Sakamoto, Selective edge lithography for fabricating imprint molds with mixed scale patterns, *J. Vacu. Sci. & Techn. B, Nanotechnol. and Microelectro.: Mater., Process., Measure., and Phenomena.* 31 (6) (2013) 06FB03.
- [151] S. Dhuey, C. Peroz, D. Olynick, G. Calafiore, S. Cabrini, Obtaining nanoimprint template gratings with 10 nm half-pitch by atomic layer deposition enabled spacer double patterning, *Nanotechnol* 24 (10) (2013) 105303.
- [152] S. Dallorto, D. Staaks, A. Schwartzberg, X. Yang, K.Y. Lee, I.W. Rangelow, S. Cabrini, D.L. Olynick, Atomic layer deposition for spacer defined double patterning of sub-10 nm titanium dioxide features, *Nanotechnol* 29 (40) (2018) 405302.
- [153] J. Zhang, X. Wang, X. Wang, H. Ma, K. Cheng, Z. Fan, Y. Li, A. Ji, F. Yang, Fully lithography independent fabrication of nanogap electrodes for lateral phase-change random access memory application, *Appl. Phys. Lett.* 96 (21) (2010) 213505.
- [154] D.C. Bien, H.W. Lee, S.A.M. Badaruddin, Formation of silicon nanostructures with a combination of spacer technology and deep reactive ion etching, *Nanoscale Res. Lett.* 7 (1) (2012) 288.
- [155] F.T. Chen, W.S. Chen, M.J. Tsai, T.K. Ku, Sidewall profile engineering for the reduction of cut exposures in self-aligned pitch division patterning, *J. Micro/Nanolithogr. MEMS MOEMS* 13 (1) (2014) 011008.
- [156] E. Cheng, H. Zou, Z. Yin, P. Jurčíček, X. Zhang, Fabrication of 2D polymer nanochannels by sidewall lithography and hot embossing, *J. Micromech. Microeng.* 23 (7) (2013) 075022.
- [157] J. Sakamoto, H. Noma, N. Fujikawa, H. Kawata, M. Yasuda, Y. Hirai, Strength enhancement of nano patterns from edge lithography for nanoimprint mold, *Microelectron. Eng.* 98 (2012) 189–193.
- [158] F. Demami, L. Ni, R. Rogel, A.C. Salaun, L. Pichon, Silicon nanowires based resistors as gas sensors, *Sensors Actuators B Chem.* 170 (2012) 158–162.
- [159] J.M. McLellan, M. Geissler, Y. Xia, Edge spreading lithography and its application to the fabrication of mesoscopic gold and silver rings, *J. Am. Chem. Soc.* 126 (35) (2004) 10830–10831.
- [160] M. Geissler, P. Chalsani, N.S. Cameron, T. Veres, Patterning of chemical gradients with submicrometer resolution using edge-spreading lithography, *Small* 2 (6) (2006) 760–765.
- [161] M.T. Zin, H.L. Yip, N.Y. Wong, H. Ma, A.K.Y. Jen, Arrays of covalently bonded single gold nanoparticles on thiolated molecular assemblies, *Langmuir* 22 (14) (2006) 6346–6351.
- [162] D. Ho, J. Zou, B. Zdyrko, K.S. Iyer, I. Luzinov, Capillary force lithography: the versatility of this facile approach in developing nanoscale applications, *Nanoscale* 7 (2) (2015) 401–414.
- [163] I. Korczagin, S. Golze, M.A. Hempenius, G.J. Vancso, Surface micropatterning and lithography with poly (ferrocenylmethylphenylsilane), *Chem. Mater.* 15 (19) (2003) 3663–3668.
- [164] X. Yu, Z. Wang, R. Xing, S. Luan, Y. Han, Solvent assisted capillary force lithography, *Polym* 46 (24) (2005) 11099–11103.
- [165] J.M. Jung, F. Stellacci, H.T. Jung, Generation of various complex patterned structures from a single ellipsoidal dot prepattern by capillary force lithography, *Adv. Mater.* 19 (24) (2007) 4392–4398.
- [166] B. Wang, Y. Hong, J. Feng, Y. Gong, C. Gao, Rings of hydrogel fabricated by a Micro-transfer technique, *Macromol. Rapid Commun.* 28 (5) (2007) 567–571.
- [167] M. Bayati, P. Patoka, M. Giersig, E.R. Savinova, An approach to fabrication of metal nanoring arrays, *Langmuir* 26 (5) (2010) 3549–3554.
- [168] Y. Cai, Z. Zhao, J. Chen, T. Yang, P.S. Cremer, Deflected capillary force lithography, *ACS Nano* 6 (2) (2012) 1548–1556.
- [169] K.H. Lee, S.M. Kim, H. Jeong, G.Y. Jung, Spontaneous nanoscale polymer solution patterning using solvent evaporation driven double-dewetting edge lithography, *Soft Matter* 8 (2) (2012) 465–471.
- [170] Z. Zhao, Y. Cai, W.S. Liao, P.S. Cremer, Stepwise molding, etching, and imprinting to form libraries of nanopatterned substrates, *Langmuir* 29 (22) (2013) 6737–6745.
- [171] M.Q. Xue, Y.L. Yang, T.B. Cao, Well-positioned metallic nanostructures fabricated by Nanotransfer edge printing, *Adv. Mater.* 20 (3) (2008) 596–600.
- [172] H.W. Ra, K.S. Choi, J.H. Kim, Y.B. Hahn, Y.H. Im, Fabrication of ZnO nanowires using nanoscale spacer lithography for gas sensors, *Small* 4 (8) (2008) 1105–1109.
- [173] Y. Li, X. Zhang, D. Wang, F. He, C. Ni, L. Chi, Fabricating sub-100 nm conducting polymer nanowires by edge nanoimprint lithography, *J. Colloid Interface Sci.* 458 (2015) 300–304.
- [174] J. Zou, B. Zdyrko, I. Luzinov, C.L. Raston, K.S. Iyer, Regiospecific linear assembly of Pd nanocubes for hydrogen gas sensing, *Chem. Commun.* 48 (7) (2012) 1033–1035.
- [175] J. Lee, W. Shim, E. Lee, J.S. Noh, W. Lee, Highly mobile palladium thin films on an elastomeric substrate: Nanogap-based hydrogen gas sensors, *Angew. Chem. Int. Ed.* 50 (23) (2011) 5301–5305.
- [176] R. Kumar, D. Varandani, B.R. Mehta, V.N. Singh, Z. Wen, X. Feng, K. Müllen, Fast response and recovery of hydrogen sensing in Pd-Pt nanoparticle-graphene composite layers, *Nanotechnol* 22 (27) (2011) 275719.
- [177] W.T. Koo, S. Qiao, A.F. Ogata, G. Jha, J.S. Jang, V.T. Chen, I.D. Kim, R.M. Penner, Accelerating palladium nanowire H2 sensors using engineered nanofiltration, *ACS Nano* 11 (9) (2017) 9276–9285.
- [178] R.M. Penner, A nose for hydrogen gas: fast, sensitive H2 sensors using electrodeposited nanomaterials, *Acc. Chem. Res.* 50 (8) (2017) 1902–1910.
- [179] X. Li, Y. Liu, J.C. Hemminger, R.M. Penner, Catalytically activated palladium@platinum nanowires for accelerated hydrogen gas detection, *ACS Nano* 9 (3) (2015) 3215–3225.
- [180] M. Schuler, N. Helwig, A. Schutze, T. Sauerwald, G. Ventura, Detecting trace-level concentrations of volatile organic compounds with metal oxide gas sensors, *Proc. IEEE* 3 (2013) 1–4.
- [181] A. Lee, B. Reedy, Temperature modulation in semiconductor gas sensing, *Sensors Actuators B Chem.* 60 (1999) 35–42.
- [182] <https://instrumentationtools.com/mos-type-gas-sensor-principle/>.
- [183] X. Zhou, X. Cheng, Y. Zhu, A.A. Elzatory, A. Alghamdi, Y. Deng, D. Zhao, Ordered porous metal oxide semiconductors for gas sensing, *Chin. Chem. Lett.* 29 (2018) 405–416.
- [184] H.J. Kim, J.H. Lee, Highly sensitive and selective gas sensors using p-type oxide semiconductors: overview, *Sensors Actuators B Chem.* 192 (2014) 607–627.
- [185] W.S. Carvalho, M. Wei, N. Ikpo, Y. Gao, M.J. Serpe, Polymer-Based Technologies for Sensing Applications, *Anal. Chem.* 90 (2017) 459–479.
- [186] Zhao, W.; Al-Nasser, L.F.; Shan, S.; Li, J.; Skeete, Z.; Kang, N.; Luo, J.; Lu, S.; Zhong, C.J.; Grausgruber, C.J.; et al. Detection of mixed volatile organic compounds and lung cancer breaths using chemiresistor arrays with crosslinked nanoparticle thin films. *Sensors Actuators B Chem.* 2016, 232, 292–299.
- [187] A. Ghoorchian, N. Alizadeh, Chemiresistor gas sensor based on sulfonated dye-doped modified conducting polypyrrole film for high sensitive detection of 2, 4, 6-trinitrotoluene in air, *Sensors Actuators B Chem.* 255 (2018) 826–835.
- [188] I.V. Zaporotskova, N.P. Boroznina, Y.N. Parkhomenko, L.V. Kozhitov, Carbon nanotubes: Sensor properties, A review. *Mod. Electron. Mater.* 2 (2016) 95–105.
- [189] M. Penza, P.J. Martin, J.T. Yeow, in: C.-D. Kohl, T. Wagner (Eds.), *Carbon Nanotube Gas Sensors In Gas Sensing Fundamentals*, Springer, Berlin, Germany, 2014, pp. 109–174.
- [190] J.J. Adjizian, R. Leghrib, A.A. Koos, I. Suarez-Martinez, A. Crossley, P. Wagner, N. Grobert, E. Llobet, C.P. Ewels, Boron- and nitrogen-doped multi-wall carbon nanotubes for gas detection, *Carbon* 66 (2014) 662–673.
- [191] H.J. Lee, K.K. Park, M. Kupnik, B.T. Khuri-Yakub, Functionalization layers for CO2 sensing using capacitive micromachined ultrasonic transducers, *Sensors Actuators B Chem.* 174 (2012) 87–93.
- [192] J. Tang, J. Fang, Y. Liang, B. Zhang, Y. Luo, X. Liu, Z. Li, X. Cai, J. Xian, H. Lin, et al., All-fiber-optic VOC gas sensor based on side-polished fiber wavelength selectively coupled with cholesteric liquid crystal film, *Sensors Actuators B Chem.* 273 (2018) 1816–1826.

- [193] S. Narasimman, L. Balakrishnan, S. Meher, R. Sivacoumar, Z. Alex, ZnO nanoparticles based fiber optic gas sensor, *AIP Conf. Proc.* 1731 (2016) 050052.
- [194] A. Paliwal, A. Sharma, M. Tomar, V. Gupta, Carbon monoxide (CO) optical gas sensor based on ZnO thin films, *Sensors Actuators B Chem.* 250 (2017) 679–685.
- [195] T. Natsuki, J.-X. Shi, Q.-Q. Ni, Vibration analysis of nanomechanical mass sensor using double-layered graphene sheets resonators, *J. Appl. Phys.* 114 (9) (2013). Article ID 094307.
- [196] Q.-T. Vien, M. O. Agyeman, T. A. Le, and T. Mak, “On the nanocommunications at THz band in graphene-enabled wireless network-on-chip,” *Math. Probl. Eng.*, vol. 2017, Article ID 9768604, 13 pages, 2017.
- [197] A.K. Naik, M.S. Hanay, W.K. Hiebert, X.L. Feng, M.L. Roukes, Towards single-molecule nanomechanical mass spectrometry, *Nat. Nanotechnol.* 4 (7) (2009) 445–450.
- [198] K. Jensen, K. Kim, A. Zettl, An atomic-resolution nanomechanical mass sensor, *Nat. Nanotechnol.* 3 (9) (2008) 533–537.
- [199] T.P. Burg, M. Godin, S.M. Knudsen, et al., Weighing of biomolecules, single cells and single nanoparticles in fluid, *Nature* 446 (7139) (2007) 1066–1069.
- [200] H. Arjmandi-Tash, A. Allain, Z. Han, V. Bouchiat, Large scale integration of CVD-graphene based NEMS with narrow distribution of resonance parameters, *2D Materials* vol. 4 (2) (2017). Article ID 025023.
- [201] D. Miller, B. Alemán, Shape tailoring to enhance and tune the properties of graphene nanomechanical resonators, *2D Materials* vol. 4 (2) (2017). Article ID 025101.
- [202] S.S. Varghese, S. Lonkar, K.K. Singh, S. Swaminathan, A. Abdala, Recent advances in graphene based gas sensors, *Sensors Actuators B Chem.* 218 (2015) 160–183.